intracellular factor(s) or event(s) are associated with activation of Syk and p38 MAP kinase in particulate-activated macrophages.

We have herein shown that *Nalp3*$^{-/-}$ and *Casp1*$^{-/-}$ mice produce similar amounts of OVA-IgE to WT mice. These results suggest that NALP3 inflammasome-dependent cytokines, such as IL-1β and IL-18, are not required for particulate-induced IgE responses. Our data in this study demonstrate that inflammasome activation and PGE_2 production are not required for the induction of antigen-specific IgG1 and IgG2c production. We found that treatment of macrophages with PVNO suppressed the production of PGE_2; however, a previous study has reported that treatment with PVNO prevent the adjuvant effect of silica on both IgE and IgG1 antibody production in vivo (Mancino et al., 1983). Taken together, these reports and our findings suggest that factor(s) induced by phagosomal destabilization other than IL-1β, IL-18, and PGE_2 are also associated with alum and silica adjuvanticity. Furthermore, these results also suggest that the properties of individual particulates are very important for the control of acquired immune responses when particulates are used as adjuvants.

The effect of PGE_2 on Th1 and Th2 cell responses is a complex issue. Previous studies have reported that PGE_2 induces type 2 immunity by suppressing the production of cytokines from Th1 cells, macrophages, and DCs (Koga et al., 2009; Kuroda and Yamashita, 2003; Fabricius et al., 2010). However, PGE_2 facilitates the differentiation of Th1 cells in the presence of IL-12 and high doses of CD28 antibody through the activation of the PI3-kinase pathway (Yao et al., 2009). Why does PGE_2 function as an activator of Th1 and Th2 cells? We speculate that the cytokine milieu, containing IL-4 and IL-12, among many other cytokines, influences the effects of PGE_2 on the immune systems. PGE_2 facilitates Th1 cell responses in the presence of IL-12 (Yao et al., 2009). In contrast, herein we show that silica and alum induce macrophages to produce only caspase-1-dependent cytokines and PGE_2, but not other inflammatory cytokines, including IL-12. Similar to the findings of others (Fedyk and Phipps, 1996; Roper et al., 1995), our findings also showed that PGE_2 cooperates with IL-4 to promote IgE production in spleen cells in vitro. Our results suggest that PGE_2 facilitates the generation of either Th1 or Th2 cell responses, depending on the balance of IL-12 and IL-4 amounts.

Our in vivo and in vitro experiments suggest that PGE_2 functions as an activator of IgE production in B cells. Consistent with these results, previous reports have shown that PGE_2 facilitates IgE production in LPS plus IL-4-stimulated B cells (Fedyk and Phipps, 1996; Roper et al., 1995). However, contrary to our findings, Garrone et al. showed that PGE_2 suppresses IgE production in anti-CD40 plus IL-4-stimulated B cells (Garrone et al., 1994). This discrepancy between their results and ours might be due to the different types of cells used. We carried out our experiments with unsorted spleen cells, but Garrone et al. used purified B cells (Garrone et al., 1994). Our findings suggest that non-B cells affected by PGE_2 might stimulate B cells to induce IgE.

In conclusion, we have found that silica and alum stimulate macrophages to produce PGE_2 through a pathway that is dependent on Syk and p38 MAP kinase. PGE_2 generated by this mechanism regulates type 2 immune responses in vivo. Our results suggest that manipulating particulate-induced cytokines and PGE_2 production could open new possibilities for the treatment of allergic inflammation, infectious diseases, and cancer.

EXPERIMENTAL PROCEDURES

Animals

Female C57BL/6 and BALB/c mice were purchased from Charles River Laboratories Japan (Yokohama, Japan). *Ptges*$^{-/-}$ mice were generated by S. Uematsu and S. Akira at Osaka University (Uematsu et al., 2002) and were backcrossed to the C57BL/6 background for five generations; their WT littermates were used as controls. *Ptgds*$^{-/-}$ mice (BALB/c background) were established by Y. Urade at the Osaka Bioscience Institute (Mohri et al., 2006). *Asc*$^{-/-}$, *Nalp3*$^{-/-}$ and *Casp1*$^{-/-}$ mice on C57BL/6 background were described previously (Mariathasan et al., 2004, 2006). *IL1r1*$^{-/-}$ mice were obtained from Jackson Laboratories. All the animal experiments were carried out in accordance to the guidelines for the care and use of animals approved by the University of Occupational and Environmental Health.

Reagents

We used three different types of alum compounds in this study. LSL alum was purchased from Cosmo Bio Co. Ltd. (Tokyo, Japan); alhydrogel was purchased from Sigma Aldrich (St. Louis, MO); and Imject alum was purchased from Pierce (Rockford, IL). All the cytokines except IL-18 were purchased from PeproTech (Rocky Hill, NJ). Recombinant mouse IL-18 and the mouse IL-18 ELISA kit were purchased from MBL (Nagoya, Japan). The cytokine and chemokine ELISA kits were purchased from PeproTech. The PGE_2 and PGD_2-MOX EIA kits were purchased from Cayman Chemical (Ann Arbor, MI). The silica crystals (Min-u-sil 5 silica) were purchased from U.S. Silica (Berkeley Springs, WV). NiO was purchased from Vacuum Metallurgical (Chiba, Japan). TiO_2 and ATP were purchased from Wako Chemical (Osaka, Japan). The PI3 kinase inhibitor wortmannin was purchased from Sigma Aldrich. The caspase-1 inhibitor I (YVAD-CHO), cathepsin B inhibitor (CA-074 Me), p38 MAP kinase inhibitor (SB203580), cyclosporine A, MEK1/2 (Erk) inhibitor (U0126), rapamycin, JNK inhibitor (SP600125), NF-κB inhibitor (wedelolactone), and Syk inhibitor were purchased from Calbiochem (Merck; Darmstadt, Germany). Cytochalasin D was purchased from Enzo Life Science (Plymouth Meeting, PA). Cytosolic PLA_2 inhibitor (Arachidonyl Trifluoromethyl Ketone) was purchased from Cayman Chemical. Leu-Leu-OMe was purchased from Chem-Impex International (Wood Dale, IL). Poly-2-vinylpyridine N-oxide (PVNO) was purchased from Polysciences (Warrington, PA). The following antibodies were used for western blot analysis: anti-GAPDH (Fitzgerald Industries International, Concord, MA); anti-COX-2 and anti-PTGES (mPGES-1) (Cayman Chemical); and anti-p38 MAP kinase and anti-phospho-p38 MAP kinase (Thr180/Tyr182) (Cell Signaling, Danvers, MA). The cells were cultured in RPMI 1640 medium (Nissui Pharmaceutical, Tokyo, Japan) supplemented with 10% FBS (BioWhittaker, Walkersville, MD, USA), 2 mM glutamine, 50 U/ml penicillin, and 50 μg/ml streptomycin (all from Life Technologies, Rockville, MD, USA).

Cell Preparation

Peritoneal macrophages were generated by injecting mice i.p. with 2 ml 4% thioglycolate broth (Eiken, Tokyo, Japan) and harvested as described previously (Kuroda and Yamashita, 2003). BM-derived macrophages were prepared by culturing BM cells in the presence of 10 ng/ml of M-CSF or GM-CSF as described previously (Kuroda et al., 2007; Kuroda et al., 2009). The purity of the BM-derived macrophages was more than 95% F4/80 and Mac-1 positive as determined by flow cytometric analysis. BM-derived DCs were prepared by culturing BM cells in the presence of 10 ng/ml of GM-CSF for 5 days. $CD11c^+$ cells were then enriched from the culture with the MACS (Miltenyi Biotec, Bergisch Gladbach, Germany). The enriched $CD11c^+$ BM-derived DCs were 80% CD11c pure, as determined by flow cytometry. Human PBMC were purified by density gradient using Lymphoprep (Axis-Sheld Poc AS, Oslo, Norway).

In Vitro Stimulation

In all the experiments, the cells were cultured at a density of 5×10^5/ml/well in 24-well plates (Falcom 3047; BD Biosciences, Franklin Lake, NJ), unless

otherwise specified. Macrophages and BM-derived DCs were primed with or without 1 ng/ml LPS (low dose) for 3 hr and then stimulated with 50 or 100 μg/ml silica, 200 or 400 μg/ml alum, 1 mM ATP, 50 or 100 μg/ml TiO_2, or 50 or 100 μg/ml NiO for 2, 6, or 18 hr. In other experiments, 10 ng/ml of IL-1 or IL-18 or 1 or 2 mM of Leu-Leu-OMe was used instead of silica or alum. In some experiments, inhibitors were added to LPS-primed macrophages together with silica, alum, or ATP. The working concentrations of the inhibitors used were as follows: 10 μM caspase-1 inhibitor I, 10 μM CA-074 Me, 2 μM cytochalasin D, 1 μM NS-398, 10 μM SB203580, 100 nM wortmannin, 100 nM cyclosporin A, 10 μM U0126, 100 nM rapamycin, 10 μM SP600125, 20 μM wedelolactone, 10 μM $cPLA_2$ inhibitor, and 1 μM Syk inhibitor. After stimulation, cell-free supernatants were collected and used for ELISA. In some experiments, macrophages stimulated with 1 μg/ml LPS (high dose) for 6 hr were used as controls. For the PVNO treatment, macrophages were incubated with or without PVNO for 5 hr. Cells were washed and then primed with low-dose LPS. LPS-primed macrophages were stimulated with silica. For the western blot analysis, LPS-primed macrophages were stimulated with silica, alum, or ATP for 30 and 60 min. The cells were then lysed with RIPA lysis buffer and used for western blot analysis as described previously (Kuroda et al., 2009). Human PBMCs were cultured at a density of 1×10^6/ml/well in 24-well plates and primed with 0.1 ng/ml LPS for 3 hr. Primed PBMC were then stimulated with 50 μg/ml silica for 3 hr.

Immunization

The mice were immunized twice (day 0 and 7) i.p. with 100 μg OVA plus 2 mg alum, 100 μg OVA plus 0.5 mg silica or 100 μg OVA plus 0.5 mg NiO in 200 μl of PBS. Ten days after the last immunization, sera were collected and analyzed for the OVA-specific IgE, IgG1, and IgG2c antibodies by ELISA.

ELISA

The amounts of cytokines, chemokines, and PGs were measured with either cytokine/chemokine ELISA kits or PGE_2/PGD_2 EIA kit in accordance with the manufacturer's instructions. The amounts of OVA-IgE in the sera were determined with the DS mouse IgE ELISA (OVA) kit (DS Pharma Biochemical, Osaka, Japan). For the analysis of OVA-IgG1 and IgG2c, serial dilutions of sera were prepared in 96-well plates coated with 10 μg/ml OVA. HRP-conjugated goat anti-mouse IgG1 or IgG2c (Bethyl Laboratories, Montgomery, TX) were used as secondary antibodies. The reciprocal value of serum dilution being absorbance (OD 405 nm) at 0.5 was defined as the titer of antigen-specific serum IgG1 and IgG2c.

Statistical analysis

All the experiments were repeated between two to five times and representative results are shown. The statistical analyses were performed with the Student's t test. p values of < 0.05 were considered statistically significant and marked with an asterisk.

SUPPLEMENTAL INFORMATION

Supplemental Information includes five figures and Supplemental Experimental Procedures and can be found with this article online at doi:10.1016/j.immuni.2011.03.019.

ACKNOWLEDGMENTS

We thank G. Krystal (British Columbia Cancer Research Agency) for helpful discussion. This work was supported in part by a UOEH Research Grant for Promotion of Occupational Health (to E.K.) and a Grant-in-Aid for Scientific Research from the Ministry of Education, Science, Sports and Culture of Japan (21890297 and 22791094 to E.K.).

Received: June 10, 2010
Revised: March 14, 2011
Accepted: March 24, 2011
Published online: April 14, 2011

REFERENCES

Aimanianda, V., Haensler, J., Lacroix-Desmazes, S., Kaveri, S.V., and Bayry, J. (2009). Novel cellular and molecular mechanisms of induction of immune responses by aluminum adjuvants. Trends Pharmacol. Sci. *30*, 287–295.

Akira, S., Uematsu, S., and Takeuchi, O. (2006). Pathogen recognition and innate immunity. Cell *124*, 783–801.

Allison, A.C., Harington, J.S., and Birbeck, M. (1966). An examination of the cytotoxic effects of silica on macrophages. J. Exp. Med. *124*, 141–154.

Boniface, K., Bak-Jensen, K.S., Li, Y., Blumenschein, W.M., McGeachy, M.J., McClanahan, T.K., McKenzie, B.S., Kastelein, R.A., Cua, D.J., and de Waal Malefyt, R. (2009). Prostaglandin E2 regulates Th17 cell differentiation and function through cyclic AMP and EP2/EP4 receptor signaling. J. Exp. Med. *206*, 535–548.

Cassel, S.L., Eisenbarth, S.C., Iyer, S.S., Sadler, J.J., Colegio, O.R., Tephly, L.A., Carter, A.B., Rothman, P.B., Flavell, R.A., and Sutterwala, F.S. (2008). The Nalp3 inflammasome is essential for the development of silicosis. Proc. Natl. Acad. Sci. USA *105*, 9035–9040.

Dinarello, C.A. (2002). The IL-1 family and inflammatory diseases. Clin. Exp. Rheumatol. ***20*** (5, Suppl 27), S1–S13.

Dostert, C., Pétrilli, V., Van Bruggen, R., Steele, C., Mossman, B.T., and Tschopp, J. (2008). Innate immune activation through Nalp3 inflammasome sensing of asbestos and silica. Science *320*, 674–677.

Duewell, P., Kono, H., Rayner, K.J., Sirois, C.M., Vladimer, G., Bauernfeind, F.G., Abela, G.S., Franchi, L., Nuñez, G., Schnurr, M., et al. (2010). NLRP3 inflammasomes are required for atherogenesis and activated by cholesterol crystals. Nature *464*, 1357–1361.

Duncan, J.A., Gao, X., Huang, M.T., O'Connor, B.P., Thomas, C.E., Willingham, S.B., Bergstralh, D.T., Jarvis, G.A., Sparling, P.F., and Ting, J.P. (2009). *Neisseria gonorrhoeae* activates the proteinase cathepsin B to mediate the signaling activities of the NLRP3 and ASC-containing inflammasome. J. Immunol. *182*, 6460–6469.

Eisenbarth, S.C., Colegio, O.R., O'Connor, W., Sutterwala, F.S., and Flavell, R.A. (2008). Crucial role for the Nalp3 inflammasome in the immunostimulatory properties of aluminium adjuvants. Nature *453*, 1122–1126.

Fabricius, D., Neubauer, M., Mandel, B., Schütz, C., Viardot, A., Vollmer, A., Jahrsdörfer, B., and Debatin, K.M. (2010). Prostaglandin E_2 inhibits IFN-α secretion and Th1 costimulation by human plasmacytoid dendritic cells via E-prostanoid 2 and E-prostanoid 4 receptor engagement. J. Immunol. *184*, 677–684.

Fedyk, E.R., and Phipps, R.P. (1996). Prostaglandin E_2 receptors of the EP2 and EP4 subtypes regulate activation and differentiation of mouse B lymphocytes to IgE-secreting cells. Proc. Natl. Acad. Sci. USA *93*, 10978–10983.

Franchi, L., and Núñez, G. (2008). The Nlrp3 inflammasome is critical for aluminium hydroxide-mediated IL-1β secretion but dispensable for adjuvant activity. Eur. J. Immunol. *38*, 2085–2089.

Franchi, L., Eigenbrod, T., Muñoz-Planillo, R., and Nuñez, G. (2009). The inflammasome: A caspase-1-activation platform that regulates immune responses and disease pathogenesis. Nat. Immunol. *10*, 241–247.

Garrone, P., Galibert, L., Rousset, F., Fu, S.M., and Banchereau, J. (1994). Regulatory effects of prostaglandin E2 on the growth and differentiation of human B lymphocytes activated through their CD40 antigen. J. Immunol. *152*, 4282–4290.

Ghiringhelli, F., Apetoh, L., Tesniere, A., Aymeric, L., Ma, Y., Ortiz, C., Vermaelen, K., Panaretakis, T., Mignot, G., Ullrich, E., et al. (2009). Activation of the NLRP3 inflammasome in dendritic cells induces IL-1β-dependent adaptive immunity against tumors. Nat. Med. *15*, 1170–1178.

Gijón, M.A., Spencer, D.M., Siddiqi, A.R., Bonventre, J.V., and Leslie, C.C. (2000). Cytosolic phopholipase A_2 is required for macrophage arachidonic acid release by agonists that do and do not mobilize calcium. J. Biol. Chem. *275*, 20146–20156.

Gordon, T.P., Kowanko, I.C., James, M., and Roberts-Thomson, P.J. (1985). Monosodium urate crystal-induced prostaglandin synthesis in the rat subcutaneous air pouch. Clin. Exp. Rheumatol. *3*, 291–296.

Gross, O., Poeck, H., Bscheider, M., Dostert, C., Hannesschläger, N., Endres, S., Hartmann, G., Tardivel, A., Schweighoffer, E., Tybulewicz, V., et al. (2009). Syk kinase signalling couples to the Nlrp3 inflammasome for anti-fungal host defence. Nature *459*, 433–436.

Halle, A., Hornung, V., Petzold, G.C., Stewart, C.R., Monks, B.G., Reinheckel, T., Fitzgerald, K.A., Latz, E., Moore, K.J., and Golenbock, D.T. (2008). The NALP3 inflammasome is involved in the innate immune response to amyloid-β. Nat. Immunol. *9*, 857–865.

Hazama, R., Qu, X., Yokoyama, K., Tanaka, C., Kinoshita, E., He, J., Takahashi, S., Tohyama, K., Yamamura, H., and Tohyama, Y. (2009). ATP-induced osteoclast function: The formation of sealing-zone like structure and the secretion of lytic granules via microtubule-deacetylation under the control of Syk. Genes Cells *14*, 871–884.

He, J., Takano, T., Ding, J., Gao, S., Noda, C., Sada, K., Yanagi, S., and Yamamura, H. (2002). Syk is required for p38 activation and G2/M arrest in B cells exposed to oxidative stress. Antioxid. Redox Signal. *4*, 509–515.

Hornung, V., Bauernfeind, F., Halle, A., Samstad, E.O., Kono, H., Rock, K.L., Fitzgerald, K.A., and Latz, E. (2008). Silica crystals and aluminum salts activate the NALP3 inflammasome through phagosomal destabilization. Nat. Immunol. *9*, 847–856.

Koga, K., Takaesu, G., Yoshida, R., Nakaya, M., Kobayashi, T., Kinjyo, I., and Yoshimura, A. (2009). Cyclic adenosine monophosphate suppresses the transcription of proinflammatory cytokines via the phosphorylated c-Fos protein. Immunity *30*, 372–383.

Kool, M., Pétrilli, V., De Smedt, T., Rolaz, A., Hammad, H., van Nimwegen, M., Bergen, I.M., Castillo, R., Lambrecht, B.N., and Tschopp, J. (2008). Cutting edge: Alum adjuvant stimulates inflammatory dendritic cells through activation of the NALP3 inflammasome. J. Immunol. *181*, 3755–3759.

Kumar, H., Kumagai, Y., Tsuchida, T., Koenig, P.A., Satoh, T., Guo, Z., Jang, M.H., Saitoh, T., Akira, S., and Kawai, T. (2009). Involvement of the NLRP3 inflammasome in innate and humoral adaptive immune responses to fungal β-glucan. J. Immunol. *183*, 8061–8067.

Kuroda, E., and Yamashita, U. (2003). Mechanisms of enhanced macrophage-mediated prostaglandin E_2 production and its suppressive role in Th1 activation in Th2-dominant BALB/c mice. J. Immunol. *170*, 757–764.

Kuroda, E., Noguchi, J., Doi, T., Uematsu, S., Akira, S., and Yamashita, U. (2007). IL-3 is an important differentiation factor for the development of prostaglandin E_2-producing macrophages between C57BL/6 and BALB/c mice. Eur. J. Immunol. *37*, 2185–2195.

Kuroda, E., Ho, V., Ruschmann, J., Antignano, F., Hamilton, M., Rauh, M.J., Antov, A., Flavell, R.A., Sly, L.M., and Krystal, G. (2009). SHIP represses the generation of IL-3-induced M2 macrophages by inhibiting IL-4 production from basophils. J. Immunol. *183*, 3652–3660.

Lee, J.K., Kim, S.H., Lewis, E.C., Azam, T., Reznikov, L.L., and Dinarello, C.A. (2004). Differences in signaling pathways by IL-1β and IL-18. Proc. Natl. Acad. Sci. USA *101*, 8815–8820.

Li, H., Willingham, S.B., Ting, J.P., and Re, F. (2008). Cutting edge: Inflammasome activation by alum and alum's adjuvant effect are mediated by NLRP3. J. Immunol. *181*, 17–21.

Mancino, D., Buono, G., Cusano, M., and Minucci, M. (1983). Adjuvant effects of a crystalline silica on IgE and IgG1 antibody production in mice and their prevention by the macrophage stabilizer poly-2-vinylpyridine N-oxide. Int. Arch. Allergy Appl. Immunol. *71*, 279–281.

Mariathasan, S., Newton, K., Monack, D.M., Vucic, D., French, D.M., Lee, W.P., Roose-Girma, M., Erickson, S., and Dixit, V.M. (2004). Differential activation of the inflammasome by caspase-1 adaptors ASC and Ipaf. Nature *430*, 213–218.

Mariathasan, S., Weiss, D.S., Newton, K., McBride, J., O'Rourke, K., Roose-Girma, M., Lee, W.P., Weinrauch, Y., Monack, D.M., and Dixit, V.M. (2006). Cryopyrin activates the inflammasome in response to toxins and ATP. Nature *440*, 228–232.

Marrack, P., McKee, A.S., and Munks, M.W. (2009). Towards an understanding of the adjuvant action of aluminium. Nat. Rev. Immunol. *9*, 287–293.

Martinon, F., Mayor, A., and Tschopp, J. (2009). The inflammasomes: Guardians of the body. Annu. Rev. Immunol. *27*, 229–265.

McKee, A.S., Munks, M.W., MacLeod, M.K., Fleenor, C.J., Van Rooijen, N., Kappler, J.W., and Marrack, P. (2009). Alum induces innate immune responses through macrophage and mast cell sensors, but these sensors are not required for alum to act as an adjuvant for specific immunity. J. Immunol. *183*, 4403–4414.

Mócsai, A., Ruland, J., and Tybulewicz, V.L. (2010). The SYK tyrosine kinase: A crucial player in diverse biological functions. Nat. Rev. Immunol. *10*, 387–402.

Mohri, I., Eguchi, N., Suzuki, K., Urade, Y., and Taniike, M. (2003). Hematopoietic prostaglandin D synthase is expressed in microglia in the developing postnatal mouse brain. Glia *42*, 263–274.

Mohri, I., Taniike, M., Taniguchi, H., Kanekiyo, T., Aritake, K., Inui, T., Fukumoto, N., Eguchi, N., Kushi, A., Sasai, H., et al. (2006). Prostaglandin D_2-mediated microglia/astrocyte interaction enhances astrogliosis and demyelination in twitcher. J. Neurosci. *26*, 4383–4393.

Narumiya, S. (2009). Prostanoids and inflammation: A new concept arising from receptor knockout mice. J. Mol. Med. *87*, 1015–1022.

Ng, G., Sharma, K., Ward, S.M., Desrosiers, M.D., Stephens, L.A., Schoel, W.M., Li, T., Lowell, C.A., Ling, C.C., Amrein, M.W., and Shi, Y. (2008). Receptor-independent, direct membrane binding leads to cell-surface lipid sorting and Syk kinase activation in dendritic cells. Immunity *29*, 807–818.

Nishi, K., Morimoto, Y., Ogami, A., Murakami, M., Myojo, T., Oyabu, T., Kadoya, C., Yamamoto, M., Todoroki, M., Hirohashi, M., et al. (2009). Expression of cytokine-induced neutrophil chemoattractant in rat lungs by intratracheal instillation of nickel oxide nanoparticles. Inhal. Toxicol. *21*, 1030–1039.

Ogami, A., Morimoto, Y., Myojo, T., Oyabu, T., Murakami, M., Todoroki, M., Nishi, K., Kadoya, C., Yamamoto, M., and Tanaka, I. (2009). Pathological features of different sizes of nickel oxide following intratracheal instillation in rats. Inhal. Toxicol. *21*, 812–818.

Roper, R.L., Brown, D.M., and Phipps, R.P. (1995). Prostaglandin E_2 promotes B lymphocyte Ig isotype switching to IgE. J. Immunol. *154*, 162–170.

Schroder, K., and Tschopp, J. (2010). The inflammasomes. Cell *140*, 821–832.

Schroder, K., Zhou, R., and Tschopp, J. (2010). The NLRP3 inflammasome: A sensor for metabolic danger? Science *327*, 296–300.

Sharp, F.A., Ruane, D., Claass, B., Creagh, E., Harris, J., Malyala, P., Singh, M., O'Hagan, D.T., Pétrilli, V., Tschopp, J., et al. (2009). Uptake of particulate vaccine adjuvants by dendritic cells activates the NALP3 inflammasome. Proc. Natl. Acad. Sci. USA *106*, 870–875.

Shio, M.T., Eisenbarth, S.C., Savaria, M., Vinet, A.F., Bellemare, M.J., Harder, K.W., Sutterwala, F.S., Bohle, D.S., Descoteaux, A., Flavell, R.A., and Olivier, M. (2009). Malarial hemozoin activates the NLRP3 inflammasome through Lyn and Syk kinases. PLoS Pathog. *5*, e1000559.

Suram, S., Brown, G.D., Ghosh, M., Gordon, S., Loper, R., Taylor, P.R., Akira, S., Uematsu, S., Williams, D.L., and Leslie, C.C. (2006). Regulation of cytosolic phospholipase A2 activation and cyclooxygenase 2 expression in macrophages by the β-glucan receptor. J. Biol. Chem. *281*, 5506–5514.

Uematsu, S., Matsumoto, M., Takeda, K., and Akira, S. (2002). Lipopolysaccharide-dependent prostaglandin $E_{(2)}$ production is regulated by the glutathione-dependent prostaglandin $E_{(2)}$ synthase gene induced by the Toll-like receptor 4/MyD88/NF-IL6 pathway. J. Immunol. *168*, 5811–5816.

Ulmann, L., Hirbec, H., and Rassendren, F. (2010). P2X4 receptors mediate PGE2 release by tissue-resident macrophages and initiate inflammatory pain. EMBO J. *29*, 2290–2300.

Von Behren, L.A., Chaudhary, S., Rabinovich, S., Shu, M.D., and Tewari, R.P. (1983). Protective effect of poly-2-vinylpyridine-N-oxide on susceptibility of silica-treated mice to experimental histoplasmosis. Infect. Immun. *42*, 818–823.

Watanabe, H., Gehrke, S., Contassot, E., Roques, S., Tschopp, J., Friedmann, P.S., French, L.E., and Gaide, O. (2008). Danger signaling through the

inflammasome acts as a master switch between tolerance and sensitization. J. Immunol. *180*, 5826–5832.

Yamamoto, M., Yaginuma, K., Tsutsui, H., Sagara, J., Guan, X., Seki, E., Yasuda, K., Yamamoto, M., Akira, S., Nakanishi, K., et al. (2004). ASC is essential for LPS-induced activation of procaspase-1 independently of TLR-associated signal adaptor molecules. Genes Cells *9*, 1055–1067.

Yao, C., Sakata, D., Esaki, Y., Li, Y., Matsuoka, T., Kuroiwa, K., Sugimoto, Y., and Narumiya, S. (2009). Prostaglandin E_2-EP4 signaling promotes immune inflammation through Th1 cell differentiation and Th17 cell expansion. Nat. Med. *15*, 633–640.

Ye, Z., and Ting, J.P. (2008). NLR, the nucleotide-binding domain leucine-rich repeat containing gene family. Curr. Opin. Immunol. *20*, 3–9.

THE JOURNAL OF IMMUNOLOGY

NLRP4 Negatively Regulates Autophagic Processes through an Association with Beclin1

Nao Jounai, Kouji Kobiyama, Masaaki Shiina, Kazuhiro Ogata, Ken J. Ishii and Fumihiko Takeshita

J Immunol 2011; 186:1646-1655; Prepublished online 5 January 2011;
doi: 10.4049/jimmunol.1001654
http://www.jimmunol.org/content/186/3/1646

The Journal of Immunology is published twice each month by
The American Association of Immunologists, Inc.,
9650 Rockville Pike, Bethesda, MD 20814-3994.

Print ISSN: 0022-1767 Online ISSN: 1550-6606.

NLRP4 Negatively Regulates Autophagic Processes through an Association with Beclin1

Nao Jounai,*,[1] Kouji Kobiyama,*,[1] Masaaki Shiina,[†] Kazuhiro Ogata,[†] Ken J. Ishii,[‡,§] and Fumihiko Takeshita*

Although more than 20 putative members have been assigned to the nucleotide-binding and oligomerization domain-like receptor (NLR) family, their physiological and biological roles, with the exception of the inflammasome, are not fully understood. In this article, we show that NLR members, such as NLRC4, NLRP3, NLRP4, and NLRP10 interact with Beclin1, an important regulator of autophagy, through their neuronal apoptosis inhibitory protein, MHC class II transcription activator, incompatibility locus protein from *Podospora anserina*, and telomerase-associated protein domain. Among such NLRs, NLRP4 had a strong affinity to the Beclin1 evolutionally conserved domain. Compromising NLRP4 via RNA interference resulted in upregulation of the autophagic process under physiological conditions and upon invasive bacterial infections, leading to enhancement of the autophagic bactericidal process of group A streptococcus. NLRP4 recruited to the subplasma membrane phagosomes containing group A streptococcus and transiently dissociated from Beclin1, suggesting that NLRP4 senses bacterial infection and permits the initiation of Beclin1-mediated autophagic responses. In addition to a role as a negative regulator of the autophagic process, NLRP4 physically associates with the class C vacuolar protein-sorting complex, thereby negatively regulating maturation of the autophagosome and endosome. Collectively, these results provide novel evidence that NLRP4, and possibly other members of the NLR family, plays a crucial role in biogenesis of the autophagosome and its maturation by the association with regulatory molecules, such as Beclin1 and the class C vacuolar protein-sorting complex. *The Journal of Immunology*, **2011, 186: 1646–1655.**

Atg5/Atg7-dependent macroautophagy (referred to as autophagy in this article), an intracellular protein-degradation system required for cellular homeostasis, regulates the sequestration and elimination of some types of intracellular bacteria (1–3). Following entry into host phagocytic cells, invasive pathogens, such as group A streptococcus (GAS; *Streptococcus pyogenes*) and *Listeria monocytogenes*, escape from the conventional phagosome by digesting its membrane with the secreted hemolytic enzymes streptolysin O and listeriolysin O, respectively (4, 5). Once bacteria are released into the cytoplasm, they are captured by the autophagosomes, whose double-membrane structure is resistant to lytic bacterial enzymes. Subsequently, the autophagosomes mature by fusion with the lysosomes, and bacteria present within autolysosomes are killed and digested. Cells that are deficient for this autophagic process are incapable of eliminating such invasive bacteria; thus, the autophagic bactericidal process is crucial for cell-autonomous antibacterial resistance.

Mechanisms underlying the initiation of autophagy have been extensively investigated over the past decade. Recent evidence indicates that one of the key initiators of the autophagic process is Beclin1, which associates with PI3K class III (PI3KC3), thereby mediating biogenesis and dynamics of subcellular membranes involved in autophagy. Additionally, it was demonstrated that binding partners of Beclin1, such as the activating molecule in Beclin1-regulated autophagy (Ambra1), UV radiation resistance-associated gene protein (UVRAG), and Atg14L, positively regulate autophagy, whereas Bcl-2, originally identified as an inhibitory factor for apoptosis signaling, inhibits autophagy (6–9). UVRAG was shown to play another biological role by interacting with the class C vacuolar protein sorting (C-VPS) complex, consisting of VPS11, VPS16 and VPS18, and facilitating the activation of Rab7 on the Rab5-labeled vacuole. This is known as Rab conversion during maturation of the autophagosome, as well as the endosome (10). Furthermore, a recent study demonstrated that Run domain protein as Beclin1 interacting and cysteine-rich containing (Rubicon) inhibits the maturation process of the autophagosome (8, 9). Taken together, it was suggested that the several

*Department of Molecular Biodefense Research, Yokohama City University Graduate School of Medicine, Yokohama 236-0004, Japan; [†]Department of Biochemistry, Yokohama City University Graduate School of Medicine, Yokohama 236-0004, Japan; [‡]Laboratory of Host Defense, World Premier International Immunology Frontier Research Center, Osaka University, Suita 565-8701, Japan; and [§]Department of Molecular Protozoology, Research Institute for Microbial Diseases, Osaka University, Suita 565-8701, Japan

[1]N.J. and K.K. contributed equally to this work.

Received for publication May 27, 2010. Accepted for publication November 30, 2010.

This work was supported in part by a grant-in-aid for scientific research from the Ministry of Education, Culture, Sports, Science, and Technology of Japan (#20590477 and #20200074 to F.T.). This work was also supported by a grant-in-aid from Yokohama Foundation for Advancement of Medical Science (to N.J.).

N.J., K.K., K.J.I., and F.T. designed the experiments; N.J., K.K., M.S., and F.T. performed the outlined research experiments; K.J.I., K.O., and F.T. analyzed data; and N.J., K.K., K.J.I., and F.T. wrote the manuscript.

Address correspondence and reprint requests to Dr. Fumihiko Takeshita, Department of Molecular Biodefense Research, Yokohama City University Graduate School of Medicine, 3-9 Fukuura Kanazawaku, Yokohama 236-0004, Japan. E-mail address: takesita@yokohama-cu.ac.jp

The online version of this article contains supplemental material.

Abbreviations used in this article: BD, Bcl-2 binding domain; CCD, coiled-coil domain; C-VPS, class C vacuolar protein sorting; ECD, evolutionally conserved domain; EGF, epidermal growth factor; EGFR, epidermal growth factor receptor; GAS, group A streptococcus; GcAV, group A streptococcus-containing autophagosome-like vacuole; MOI, multiplicity of infection; NACHT, neuronal apoptosis inhibitory protein, MHC class II transcription activator, incompatibility locus protein from *Podospora anserina*, and telomerase-associated protein; NLR, nucleotide-binding and oligomerization domain-like receptor; PI3KC3, PI3K class III; siRNA, small interfering RNA; THY medium, Todd Hewitt medium supplemented with yeast extract; UVRAG, UV radiation resistance-associated gene protein; VSV, vesicular stomatitis virus; WT, wild-type.

www.jimmunol.org/cgi/doi/10.4049/jimmunol.1001654

binding partners of Beclin1 have at least two functions during the autophagic process, thereby controlling autophagic flux. The first function seems to be control of Beclin1-mediated initiation of autophagy, and the second is control of the maturation process of the autophagosome.

Nucleotide-binding and oligomerization domain-like receptors (NLRs) are categorized as a family of cytosolic proteins having structurally conserved domains. This protein family consists of 23 putative members that have been identified in humans and 34 that have been identified in mice. According to a genome-wide analysis of the putative genes, all have several shared domains, such as neuronal apoptosis inhibitory protein, MHC class II transcription activator, incompatibility locus protein from *Podospora anserina*, and telomerase-associated protein (NACHT) domain, pyrin domain, the caspase recruitment domain, and the leucine-rich repeat domain. Some NLR family members, such as NLRC4, NLRP1, and NLRP3, were shown to form an ~700-kDa cytoplasmic protein complex, called an inflammasome, to facilitate the maturation and secretion of proinflammatory cytokines, including IL-1β, IL-18, and IL-33, in response to bacterial infections (11). It was shown that autophagy and a distinct type of cell death process, termed "pyroptosis," are upregulated in NLRC4$^{-/-}$ macrophages relative to wild-type (WT) macrophages postinfection with *Shigella*, suggesting that NLRC4 negatively regulates autophagy and the induction of cell-autonomous bactericidal processes (12).

In the current study, we examined the molecular mechanisms underlying the association between NLR family members and the Beclin1-mediated autophagic bactericidal process. Our results demonstrated that NLRC4 and NLRP4 negatively regulate autophagic processes through an association with Beclin1. In addition, NLRP4 physically interacts with the C-VPS complex, thereby blocking maturation of autophagosomes to autolysosomes. Furthermore, NLRP4 is recruited to and accumulates in the bacteria-containing phagosomes and transiently dissociates from Beclin1 after GAS infection. Our results suggested that NLRP4 is engaged in the mechanism controlling the autophagic flux crucial for the cell-autonomous antibacterial resistance.

Materials and Methods

Cells, bacteria, and reagents

HEK293, THP-1, and HeLa cells were purchased from the American Type Culture Collection. HEK293 and HeLa cells were maintained in DMEM, whereas THP-1 cells were maintained in RPMI 1640 supplemented with FCS and 50 mg/ml each penicillin and streptomycin. The normal primary HUVECs were purchased from TAKARA (Japan). HUVECs were maintained in the supplemented endothelial cell growth medium-2 without antibiotics, according to the manufacturer's instruction. GAS serotype M6 was a kind gift from E. Hanski (The Hebrew University, Hadassah Medical School, Jerusalem, Israel). GAS was cultured in Todd Hewitt medium supplemented with yeast extract (THY medium) (BD Biosciences). For infection experiments, GAS was prepared by adjusting to 1 OD_{590} (~1 × 10^9 cells/ml) and washing twice with PBS before infection. *L. monocytogenes* were grown in brain/heart infusion broth (BD Biosciences) at 37°C. For infection experiments, *L. monocytogenes* were prepared by adjusting to 1 OD_{600} (~2 × 10^9 cells/ml) and washing twice with PBS before infection. Vesicular stomatitis virus (VSV) was provided by the National Institute of Animal Health (Tokyo, Japan). Cell transfection and RNA interference were performed as described previously (13). The dsRNA for knockdown of *NLRC4* and *NLRP4* was obtained from Invitrogen (stealth RNAi). Each knockdown of *NLRC4* or *NLRP4* was performed with pooled dsRNAs whose sequences are shown in Supplemental Table I. Control small interfering RNA (siRNA) was purchased from Invitrogen (cat. #12935-300). Primers (Supplemental Table II) were used to confirm the level of RNA encoding *NLRC4* and *NLRP4*. In some cases, cotransfection with expression plasmid and siRNA was performed by Lipofectamine 2000 (Invitrogen), according to the manufacturer's instructions.

Gel-filtration assay

HeLa cells were disrupted as described previously (14), and the cytoplasmic lysate was subjected to size fractionation with Superdex 200 (GE Healthcare).

Plasmids

NLRC4, NLRP3, NLRP4, NLRP10, Beclin1, p57, VPS11, VPS16, VPS18, and LC3 cDNAs were amplified by PCR using a human or mouse spleen cDNA library. The cDNA fragments were introduced into pFLAG-CMV4, pFLAG-CMV5 (Sigma), pCIneo (Promega), pCIneo-HA, or pCAGGS-CFP (15). Each truncated protein was prepared by insertion of the following PCR amplicons into expression vector plasmids: NLRC4 caspase recruitment domain (1–100), NLRC4 NACHT (100–500), NLRP3 NACHT (200–550), NLRP4 NACHT (100–500), NLRP10 NACHT (140–500), Beclin1 BD (90–152), Beclin1 CCD (152–246), and Beclin1 ECD (246–339). To construct the mRFP-GFP-LC3–expressing plasmid, open reading frames of mRFP, GFP, and LC3 were tandemly ligated and introduced into pCIneo. For generation of recombinant lentiviruses, the targeting cDNA was introduced into CSII-CMV-MCS-IRES-puro or CSII-EF-MCS-IRES-hyg (16, 17) to obtain CS-mRFP-GFP-LC3-IRES-puro, CS-CFP-NLRP4-IRES-hyg, and CS-CFP-p57-IRES-hyg.

Immunoprecipitation and immunoblotting

Immunoprecipitation assays were performed as described previously (18). Immunoblotting analyses were performed using anti-LC3 (Cell Signaling, cat. #2775), anti-Beclin1 (AnaSpec), anti–β-actin (Cell Signaling Technology), anti-NLRC4 (AnaSpec, cat. #54128), anti-NLRP4 (IMGENEX, cat. #IMG-5743), anti-p62 (BIOMOL, cat. #PW9860), anti-FLAG M2 (Sigma), or anti-HA (Roche Diagnostics), as described previously (18). For reprobing the membrane with different Abs, the membrane was incubated in stripping buffer (400 mM glycine, 0.2% SDS, 2% Tween 20 [pH 2.2]) for 10 min at room temperature, washed, and Ab was added to the membrane. To detect human NLRC4 and NLRP4 protein, Can Get Signal (TOYOBO) was used to augment the signal.

RT-PCR

Total RNA was extracted with TRIzol reagent (Invitrogen), according to the manufacturer's instructions. Extracted total RNA was reverse transcribed with ReverTra Ace reverse transcriptase (TOYOBO), and standard PCR was conducted as described previously (19).

Quantitative RT-PCR

SYBR Green technology was applied for all of the assays with ABI 7500 standard quantitative PCR system (Applied Biosystems, CA). SYBR Premix Ex Taq II was purchased from TAKARA (Japan). Primer pairs are listed in Supplemental Table III. The *gapdh* gene was used as an internal control.

Cytokine ELISA

Human IL-1β was quantified with the Human IL-1β/IL-1F2 DuoSet (R&D Systems), according to the manufacturer's instruction.

Evaluation of bacterial viability

The bacteria grown until midlog phase were harvested and washed twice with PBS (pH 7.4) and then adjusted to appropriate cell density. The bacteria were added to cell cultures (1 × 10^5 HeLa cells or 2 × 10^5 HUVECs in a 12-well culture plate) at a multiplicity of infection (MOI) of 50 without antibiotics. One hour postinfection, antibiotics (penicillin and streptomycin) were added to the culture medium to kill extracellular bacteria, and the cells were further cultured for the indicated time periods. After an appropriate incubation time, infected cells were lysed in 1 ml sterile distilled water, and serial dilutions of the lysates were plated on THY agar plates. The colony numbers were enumerated 24 h after plating. Data represent the mean ± SD of recovered bacteria for three independent experiments.

Generation of stably transformed HeLa cells

Recombinant lentiviruses expressing mRFP-GFP-LC3, CFP-NLRP4, or CFP-p57 were generated by transfecting CS-mRFP-GFP-LC3-IRES-puro, CS-CFP-NLRP4-IRES-hyg, or CS-CFP-p57-IRES-hyg, as well as pCAG-HIVgp and pCMV-VSV-G-RSV-Rev, into HEK293 cells, as described in another study (20). Forty-eight to seventy-two hours following transfection, the culture supernatants were recovered and transferred to the fresh HeLa cell culture. HeLa cells expressing mRFP-GFP-LC3, CFP-

NLRP4, or CFP-p57 were selected in the presence of puromycin (2 mg/ml) alone or puromycin plus hygromycin (200 mg/ml).

Fluorescent and confocal microscopy analysis

Fluorescent microscopy analysis was performed with a fluorescent deconvolution microscope (BIOZERO; Keyence, Japan). Confocal microscopy analysis was performed with FLUOVIEW FV1000-D (BX61WI; OLYMPUS). For immunofluorescent staining of GAS, HeLa cells were fixed and immunostained with an anti-GAS Ab (Abcam), followed by an Alexa Fluor 546-conjugated anti-rabbit IgG (Invitrogen) secondary Ab, and were subjected to microscopy analysis.

Epidermal growth factor receptor degradation assay

Control, NLRC4-knockdown, or NLRP4-knockdown HeLa cells were treated with 200 ng/ml recombinant epidermal growth factor (EGF) (R&D Systems) for the indicated periods and were subjected to immunoblotting analysis with the anti-EGF receptor (EGFR) (1005; Santa Cruz).

Statistical analysis

The Student *t* test was used for statistical analysis.

Results

NLR family members interact with Beclin1

To assess possible roles for NLR family members in the autophagic process, their molecular interactions with Beclin1, the primary regulator of autophagy, was examined by immunoprecipitation analysis. As a result, NLRC4, NLRP3, NLRP4, NLRP10, and NOD2, but not GFP, coprecipitated with Beclin1 in HEK293 and HeLa cells, suggesting that these NLR family members have the potential to interact with Beclin1 (Fig. 1*A*, Supplemental Fig. 1*A*, 1*B*). Additionally, a NACHT domain of each NLR was shown to be sufficient for interaction with Beclin1 (Fig. 1*B*). The highest levels of such an interaction were seen between NLRP4 NACHT and Beclin1 (Fig. 1*B*). The NACHT domain of NLRC4 was shown to catalyze nucleotide hydrolysis through direct interaction with ATP/2′deoxyadenosine triphosphate, crucial for self-multimerization, caspase-1 activation, and subsequent IL-1β release as a function of the inflammasome. In contrast to such previous observations, the loss-of-function mutant NLRC4 NACHT K175R was shown to interact with Beclin1 comparably to WT NLRC4, suggesting that ATP/2′deoxyadenosine triphosphate binding is not essential for NACHT domain interaction with Beclin1 (Fig. 1*B*). We further examined the endogenous interaction between NLRP4 and Beclin1 in HeLa cells or the normal primary HUVECs. As a result, NLRP4 was shown to interact with Beclin1 under physiological conditions (Fig. 1*C*, Supplemental Fig. 2).

Although endogenous human NLRP4 protein could be recognized at the expected size upon immunoblotting, little is known about the expression of human NLRP4. To strengthen NLRP4 expression in HeLa cells and HUVECs, we evaluated *NLRP4*-encoding RNA level (Supplemental Fig. 3*A*, 3*B*). The *NLRP4*-encoding RNA could be detected in HeLa cells and HUVECs by RT-PCR (Supplemental Fig. 3*A*). To quantify *NLRP4*-encoding RNA level by quantitative PCR, we evaluated it compared with the expression level of NLRC4, because its expression at the RNA and protein levels has been reported (21). As shown in Supplemental Fig. 3*B*, the level of *NLRP4*-encoding RNA was 6-fold lower than that of *NLRC4* in HeLa cells. However, the RNA level of *NLRP4* in HUVECs was comparable to that of *NLRC4* in HeLa cells and slightly less than that of *NLRC4* in HUVECs (Supplemental Fig. 3*B*). It suggests that *NLRP4*'s expression level might vary among cell types, and *NLRP4* in HUVECs was expressed at the same RNA level as *NLRC4* in HeLa cells (Supplemental Fig. 3*B*).

Beclin1 was shown to interact with several autophagy regulators via distinct interaction domains: the Bcl-2 binding domain (BD), the coiled-coil domain (CCD), and the evolutionally conserved domain (ECD), whose structure is uncharacterized but highly conserved among Beclin1 zoologues. When each Beclin1 domain (BD, CCD, ECD) was ectopically expressed in HEK293 cells, the levels of ECD protein were relatively low (Fig. 1*D*). Nonetheless, the level of each NACHT domain that coprecipitated with Beclin1 ECD was higher than those with Beclin1 BD or CCD, suggesting that Beclin1 ECD has a high affinity for the NLR NACHT domains (Fig. 1*D*). Consistent with the result shown in Fig. 1*B*, the NLRP4 NACHT domain most strongly interacted with the Beclin1 ECD (Fig. 1*D*). Furthermore, we characterized several point mutants of the NLRP4 NACHT domain and found that NLRP4 NACHT W345A or W405A was incapable of interacting with Beclin1, suggesting that the structure conformed by these Trp residues confers the interaction between the NLRP4 NACHT domain and Beclin1 ECD (Fig. 1*E*).

It was shown that Beclin1 physiologically interacts with a variety of cytoplasmic proteins, forming different types of molecular complexes (6). To examine whether NLRP4 also forms the complexes in the cells, HeLa cells were mechanically disrupted, and the cytoplasmic lysate was size fractionated by gel filtration. The presence of Beclin1 (52 kDa) and NLRP4 (113 kDa) in each fraction was examined by immunoblotting. Beclin1 was found in fractions 3–6 comprising molecules of 400–700 kDa, consistent with a previous report (Fig. 1*F*) (8). NLRP4 was found in fractions 4 and 5, suggesting that NLRP4 might be present in the 500–700-kDa cytoplasmic complex containing Beclin1 (Fig. 1*C*, 1*F*).

The NLR NACHT domain promotes the interaction between Beclin1 and the heterologous NACHT domain

The NLR NACHT domains were suggested to play a role in self-multimer formation, which is crucial for inflammasome activation. As shown in Fig. 2*A*, FLAG-NLRP4 interacted with HA-NLRC4, HA-NLRP3, HA-NLRP4, or HA-NLRP10. Among these, FLAG-NLRP4 showed the highest levels of interaction with HA-NLRP4, suggesting that NLRP4 preferentially forms the homologous multimer. Similarly, the NACHT domains of these NLR family members were sufficient for association with the NACHT domain of NLRP4 (Fig. 2*B*). The NLRP4 NACHT W345A and W405A, which are not capable of binding to Beclin1, also interacted with the homologous WT NACHT domain (Fig. 2*B*), suggesting that the structural bases are different between NACHT–NACHT and NACHT–Beclin1 interactions. We then examined whether a multimer formation between different NLR family members modulates NLR interaction with Beclin1. Although the interaction between NLRP4 and NLRC4 was weak (Fig. 2*A*), the degree of NLRP4 interaction with Beclin1 ECD increased as a result of NLRC4 concomitantly interacting with Beclin1 ECD in a dose-dependent fashion (Fig. 2*C*). A similar result was observed involving the NACHT domains of NLRC4 and NLRP4 (Fig. 2*D*), suggesting that the NLRP4 NACHT domain facilitates the interaction between Beclin1 and the heterologous NACHT domain. We also examined whether overexpression of Beclin1 ECD leads to upregulation of autophagy by dissociating NLRP4 from Beclin1. However, as a result, neither the number of LC3 vacuoles nor the levels of p62, an intracellular protein specifically and constitutively degraded by autophagic process (22), changed following Beclin1 ECD overexpression (Supplemental Fig. 4*A*, 4*B*).

Knockdown of NLRC4 or NLRP4 promotes the autophagic process

Based on experiments investigating the association between NLR family molecules and Beclin1, NLRP4 NACHT domain showed a stronger affinity with Beclin1 ECD than other NLR NACHT

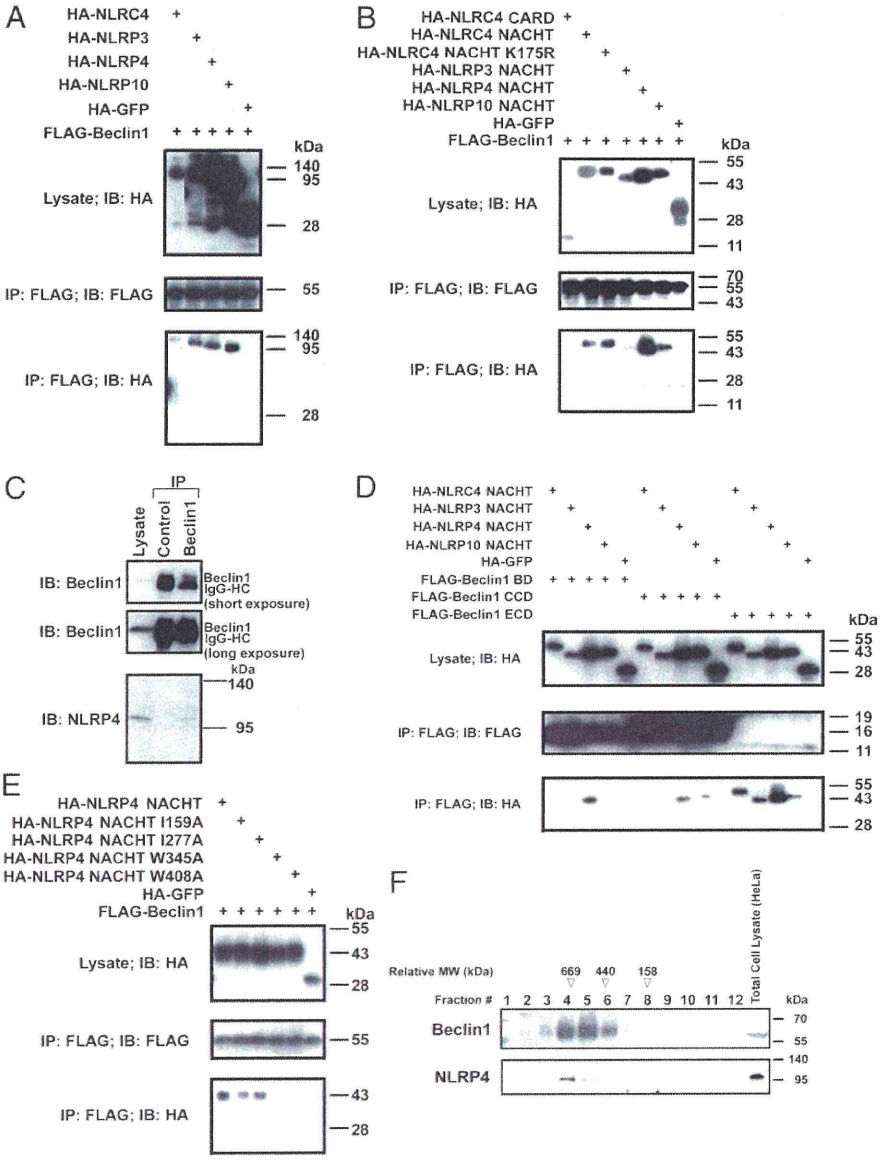

FIGURE 1. The NLR family of proteins interacts with Beclin1 through the NLR NACHT domain and Beclin1 ECD. *A*, *B*, *D*, and *E*, HEK293 cells were transfected with the indicated plasmids. Forty-eight hours posttransfection, cells were subjected to immunoprecipitation and immunoblotting analyses. *C*, Six million HeLa cells were lysed, endogenous Beclin1 was immunoprecipitated, and the associated levels of NLRP4 were immunoblotted. *F*, HeLa cells were mechanically disrupted, and the lysate was fractioned with Sephadex 200. The expression level of Beclin1 or NLRP4 in each fraction was examined by immunoblotting. Representative results from at least three independent experiments are shown.

domains (Fig. 1*B*, 1*D*), indicating that NLRP4 might strongly influence the induction and/or magnitude of autophagy. To examine the roles of NLRP4 in the autophagic process, NLRC4 or NLRP4 mRNA was ablated by RNA interference. The levels of RNA encoding endogenous NLRC4 or NLRP4 were specifically decreased by siRNA treatment in HeLa cells (Fig. 3*A*). The knockdown efficiency by NLRP4 siRNA was also confirmed at endogenous protein levels (Fig. 3*B*, Supplemental Fig. 5). To monitor the levels of the autophagic process, the levels of LC3 conversion were examined in the cells pretreated with each siRNA. Because modified LC3 (LC3-II), a hallmark of autophagy, is degraded on achievement of autophagy, the levels of LC3-II were examined in the presence of protease inhibitors pepstatin A and E64d (Fig. 3*C*). Under physiological conditions, the LC3-II levels were higher in cells treated with NLRC4 or NLRP4 siRNA relative to those with control siRNA, suggesting that the autophagic process is constitutively promoted in the cells depleted of NLRC4 or NLRP4 (Fig. 3*C*). Following invasive GAS infection, the LC3-II levels were increased in all samples, but they were greater in NLRC4- or NLRP4-knockdown cells compared with control cells (Fig. 3*C*). The influence of decreased NLRC4 or NLRP4 on autophagy was also examined with well-known autophagy inducers, such as rapamycin, VSV, and other invasive bacteria (*L. monocytogenes*) (Supplemental Fig. 6*A–C*) (18). The treatment of rapamycin or VSV infection resulted in LC3-II accumulation in NLRC4- or NLRP4-knockdown cells at a level comparable to control cells (Supplemental Fig. 6*A*, 6*B*). In contrast, *L. monocytogenes* infection resulted in the enhancement of LC3-II accumulation by the knockdown of NLRC4 or NLRP4 (Supplemental Fig. 6*C*). Collectively, the data suggested that NLRC4 or NLRP4 negatively regulates the induction of autophagy upon invasive bacterial infection (Supplemental Fig. 6*A–C*).

To further confirm the influence of NLRC4 and NLRP4 on the autophagic process, the LC3-II levels were also monitored in the absence of protease inhibitors (Fig. 3*D*). Of interest, LC3-II was barely detected in NLRP4-knockdown cells under physiological conditions and even after GAS infection (Fig. 3*D*). The levels of the other hallmark of autophagy, p62, were lower in NLRP4 knockdown cells compared with control cells before GAS infection (Fig. 3*D*). The GAS infection did not affect the levels of p62 in the cells treated with siRNA of control, NLRC4-knockdown, or NLRP4-knockdown cells, indicating that phys-

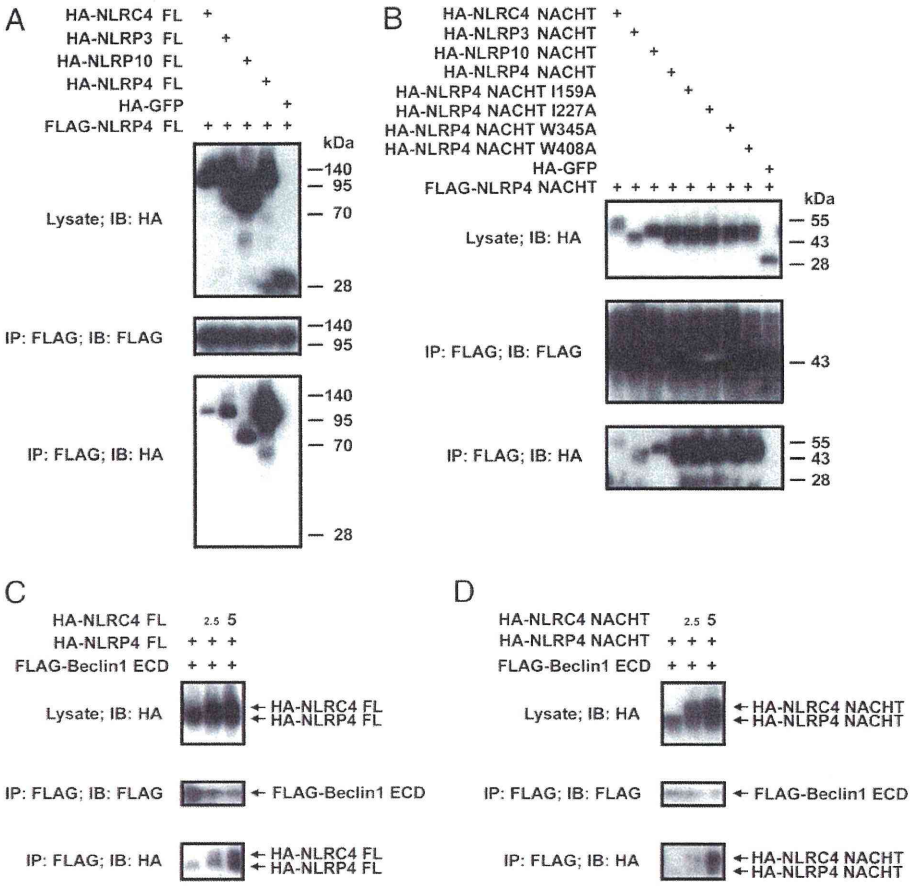

FIGURE 2. NACHT domains of NLRs are important for their oligomerization, as well as association with Beclin1. *A–D*, HEK293 cells were transfected with the indicated plasmids. Forty-eight hours posttransfection, the cells were subjected to immunoprecipitation and immunoblotting analysis. Representative results from at least three independent experiments are shown.

iological autophagy might be distinct from GAS-mediated autophagy on discrimination of substrates to degrade (Fig. 3*D*). In addition, the fluorescent microscopy analysis showed that the reduced NLRP4 resulted in greater numbers of LC3-II vacuoles under physiological conditions (Supplemental Fig. 7). These results collectively suggested that NLRC4 and NLRP4 negatively regulate the autophagic process under physiological conditions, as well as postinvasive bacterial infection, and that NLRP4, but not NLRC4, inhibits the protein-degradation process mediated by autophagy.

To examine whether the autophagic process regulated by NLRC4 or NLRP4 controls the intracellular bactericidal activity, the survival rate of intracellular bacteria was monitored following GAS infection (Fig. 3*E*). The number of bacteria that survived was significantly less in the NLRC4- or NLRP4-knockdown cells compared with control cells. Furthermore, the bacterial number was significantly less in the NLRP4-knockdown cells compared with the NLRC4-knockdown cells. Collectively, these data suggested that NLRC4 and NLRP4 negatively control the intracellular bactericidal activity, at least in part, through inhibition of the autophagic process (Fig. 3*E*).

We further investigated whether NLRP4 also functions as a negative regulator of autophagy in human primary cells, such as HUVECs. As shown in Fig. 3*F*, the knockdown of NLRP4 or NLRC4 in HUVECs resulted in accelerated autophagy after GAS infection. In addition, the reduction of NLRP4 resulted in greater bactericidal activity, suggesting that NLRP4 and NLRC4 are negative regulators of bactericide in HUVECs (Fig. 3*G*).

Some NLRs, such as NLRP3 and NLRC4, were shown to mediate the signaling leading to inflammasome activation. The secretion of IL-1β, a hallmark of inflammasome activation, was not detected in HeLa cells, even after treatment with a known inflammasome-activating agent, such as LPS, or GAS infection (Supplemental Fig. 8). Instead, the role of NLRP4 in inflammasome activation was examined by coexpression of inflammasome components: caspase-1 and apoptosis-associated speck-like protein containing a caspase recruitment domain. Coexpression of these molecules facilitated IL-1β secretion. The level of IL-1β was further increased in the presence of NLRC4 but not NLRP4, suggesting that NLRC4 is engaged, at least in part, in inflammasome activation in HeLa cells (Supplemental Fig. 8*B*).

NLRP4 is transiently recruited to bacteria-containing autophagosomes and dissociates from Beclin1 at an early stage of GAS infection

To examine whether NLRP4 controls GAS-mediated autophagosome formation, the numbers of LC3 puncta were evaluated by confocal microscopy analysis (Fig. 4*A*, 4*B*, Supplemental Fig. 9*A*). As a result, the number of GAS-associated LC3$^+$ vacuoles was greater in NLRP4-knockdown cells than in control cells, suggesting that NLRP4 negatively regulates the induction of GAS-associated LC3 vacuoles (Fig. 4*A*, 4*B*, Supplemental Fig. 9*A*). To examine the subcellular dynamics of NLRP4 upon GAS infection, HeLa cells stably expressing CFP-NLRP4 and GFP-LC3 were established. Although diffusely present in the cytoplasm under physiological conditions, NLRP4 was recruited to the subplasma membrane area close to phagosomes containing GAS 30 min postinfection (Fig. 4*C*, Supplemental Fig. 9*B*). Similar relocalization was observed when the well-characterized phagosomal marker p57, also known as TACO or coronin1, was examined (Fig. 4*D*). In contrast, NLRP4 returned to a diffuse distribution in the cytoplasm 120 min postinfection, when most bacteria were

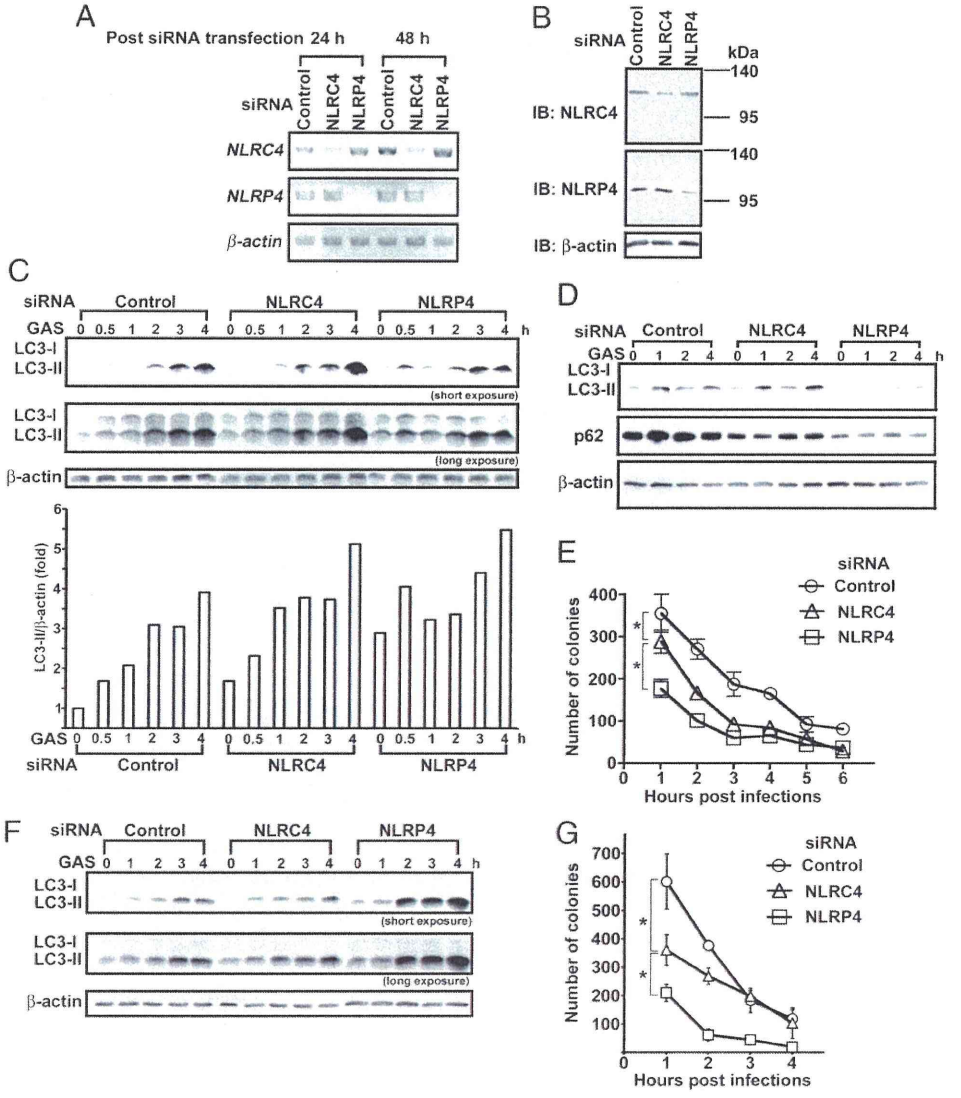

FIGURE 3. Enhancement of autophagy by repressing expression of NLRC4 or NLRP4. *A–C*, HeLa cells were transfected with control dsRNA or pooled dsRNAs targeting NLRC4 or NLRP4. *A*, Twenty-four or forty-eight hours following transfection, the mRNA levels of NLRC4, NLRP4, or β-actin were examined by RT-PCR analysis. *B*, Forty-eight hours following transfection, the protein levels of NLRC4, NLRP4, or β-actin were examined by immunoblotting. *C*, HeLa cells pretreated with siRNA were treated with protease inhibitors for 4 h and then were infected with GAS at an MOI of 50 for the indicated times. The levels of LC3-II in each sample were examined by immunoblotting analysis (*upper panel*). Band intensity was measured by Image J software. The intensity values of LC3-II were normalized to those of β-actin (*lower panel*). *D*, Cells pretreated with siRNA were infected with GAS at an MOI of 50 for the indicated times. The levels of LC3-II and p62 in each sample were examined by immunoblotting analysis. *E*, The HeLa cells were lysed in 1 ml of sterile distilled water, and 100 μl of each lysate was spread on THY agar plates ($n = 3$). The numbers of colonies were counted 24 h after incubation at 37°C. The graph shows the mean ± SD. Representative results from at least three independent experiments are shown. *F* and *G*, HUVECs pretreated with siRNA were further treated with protease inhibitors for 4 h and then infected with GAS at an MOI of 50 for the indicated times. *F*, The levels of LC3-II in each sample were examined by immunoblotting analysis. *G*, The HUVECs were lysed in 1 ml of sterile distilled water, and 100 μl of each lysate was spread on THY agar plates ($n = 3$). The numbers of colony were counted 24 h after plating. The graph shows the mean ± SD. Representative results from at least three independent experiments are shown. $^*p < 0.05$.

encapsulated by the $LC3^+$ vacuoles (i.e., autophagosomes) (Fig. 4*C*, Supplemental Fig. 9*B*). p57 remained localized in the vacuoles containing bacteria 120 min postinfection (Fig. 4*D*). We also evaluated whether the levels of interaction between NLRP4 and Beclin1 changed following GAS infection. HeLa cells were transfected with an expression plasmid encoding HA-NLRP4, and we found that HA-NLRP4 specifically interacted with endogenous Beclin1 (Fig. 4*E*). The level of interaction between HA-NLRP4 and Beclin1 decreased 60 min following GAS infection, but it returned to normal levels after 120 min (Fig. 4*E*). Because the size of Beclin1 is similar to that of an IgG H chain, the exact levels of immunoprecipitated Beclin1 could not be evaluated (Fig. 4*E*). We also found that the degrees of interaction between FLAG-NLRP4 and HA-Beclin1 decreased 30–60 min after GAS infection but returned to their original levels after 120 min (Fig. 4*F*). It was proposed that NLRP4 can detect infection by invasive bacteria, is recruited to the phagosomes, and dissociates from Beclin1, thereby permitting induction of autophagy, culminating in the induction of the intracellular bactericidal process.

NLRP4 but not NLRC4 inhibits maturation of autophagosomes

Once the autophagosome undergoes maturation and couples with lysosomes, it functions as the autolysosome, initiating the intra-

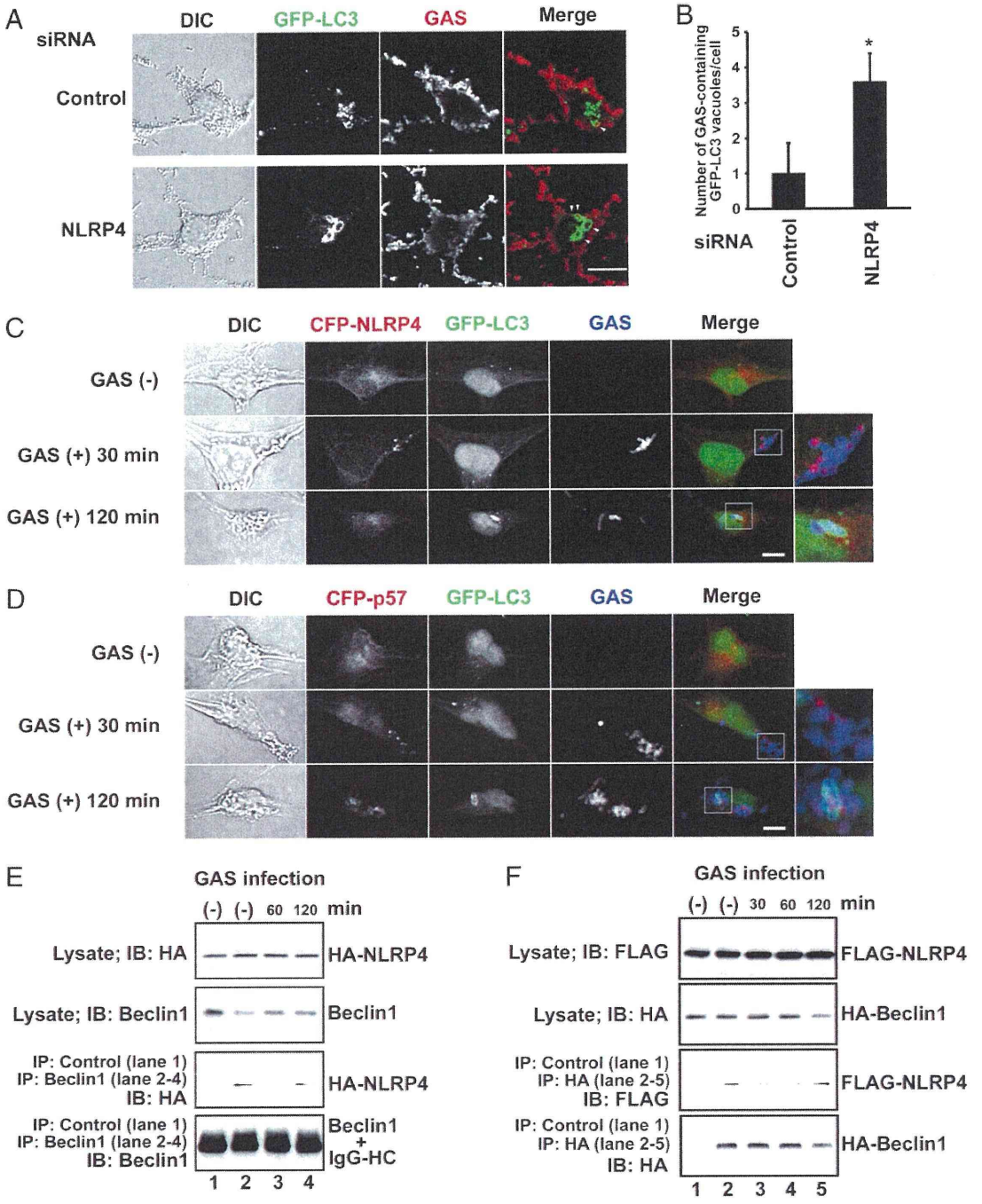

FIGURE 4. The dynamics of subcellular localization of NLRP4 and the levels of interaction between NLRP4 and Beclin1 following GAS infection. *A* and *B*, HeLa cells were cotransfected with the indicated siRNA and GFP-LC3 expression plasmid, and the cells were infected with GAS at an MOI of 100. At 2 h postinfection with GAS, the cells were fixed and immunostained with anti-GAS Ab, followed by Alexa 546-conjugated anti-rabbit Ab. The samples were subjected to confocal microscopy analysis. *A*, Representative photomicrographs from seven cells examined. Arrowheads in merge images denote GAS-associated LC3 vacuoles. Scale bar, 20 μm. *B*, The number of GAS-associated LC3 vacuoles (>2 μm) in individual cells was counted ($n = 15$). The graph shows the mean ± SD. *$p < 0.01$. HeLa cells stably expressing GFP-LC3 plus CFP-NLRP4 (*C*) or CFP-p57 (*D*) were infected with GAS at an MOI of 50 for the indicated times and then fixed. Intracellular GAS was immunostained with anti-GAS Ab, followed by Alexa Fluor 546-conjugated anti-rabbit Ab. The samples were examined under a confocal microscope. Scale bar, 20 μm. Representative photomicrographs from 10–15 cells examined. Three independent experiments gave similar results. HeLa cells were transfected with an expression plasmid for HA-NLRP4 (*E*) or FLAG-NLRP4 and HA-Beclin1 (*F*). Forty-eight hours after transfection, the cells were infected with GAS at an MOI of 50 for the indicated times. The cells were then subjected to immunoprecipitation assays. Representative results from at least three independent experiments are shown.

cellular bactericidal process. To monitor the real-time formation of autophagosomes and autolysosomes, we established a HeLa cell line that stably expressed the mRFP-GFP-LC3 fusion protein. According to a previous report (23), when this indicator protein is present in the autophagosome, the mixed fluorescence of red and green is detected as yellow. By contrast, in the autolysosome, the tertiary structure of GFP, but not that of mRFP, is disrupted because of low pH, and the indicator fluorescence is red.

Rab7, a small GTPase known to localize on the lysosome membrane, was recruited to the red fluorescent vacuoles but not to the yellow ones (data not shown). Using this indicator, we evaluated the maturation of the autophagosomes in living cells. The number of yellow vesicles was greater in NLRC4- and NLRP4-knockdown cells relative to control cells, suggesting that autophagosome formation is upregulated (Fig. 5*A*). By contrast, the number of red vesicles was significantly greater in NLRP4-knockdown cells compared with NLRC4-knockdown or control cells, indicating that the rate of autophagosome maturation is enhanced by interrupting NLRP4 expression but not NLRC4 expression (Fig. 5*A*, 5*B*). When these cells were infected with GAS, the number of yellow vesicles increased in NLRC4-knockdown cells compared with NLRP4-knockdown or control cells. Knockdown of NLRP4 seemed to accelerate the rate of autophagosome maturation, resulting in a reduction in the transient number of autophagosomes (Fig. 5*B*, 5*C*). Altogether, these results indicated that NLRC4 and NLRP4 negatively regulated the initiation of the autophagic process, whereas NLRP4, but not NLRC4, inhibited autophagosome maturation (Fig. 5*D*).

A recent study revealed that Rubicon, a negative regulator of the autophagic machinery, contains a property that is inhibitory for autophagosomal maturation because of a mechanism shared by the endosomal-maturation process, which is critically involved in EGF-dependent degradation of the EGFR. To examine whether NLRP4 has a similar property, the efficiency of EGFR degradation induced by EGF treatment was monitored by immunoblotting. As shown in Fig. 5*E*, the levels of EGFR were reduced in response to EGF treatment of HeLa cells. However, the rate of EGFR degradation was significantly greater in NLRP4-knockdown cells compared with NLRC4-knockdown or control cells. A similar result was obtained when the rate of EGFR degradation was examined using A549 cells (Supplemental Fig. 10). The formation of the autolysosome and endolysosome is mediated by the molecular mechanisms controlling tethering and fusion of vacuolar membranes. Such membrane dynamics are chiefly controlled by the C-VPS complex consisting of VPS11, VPS16, VPS18, and a small GTPase (Rab7) on the Rab5-labeled early endosomes. To examine the molecular mechanisms underlying NLRP4-mediated suppression of autophagosome maturation, the interaction between each C-VPS component and NLR family member was analyzed by immunoprecipitation (Fig. 5*F*). Significant levels of VPS11, VPS16, and VPS18 coprecipitated with NLRP4 compared with NLRC4 or control GFP, suggesting that NLRP4 has a stronger affinity for the C-VPS complex and, thereby, controlled the maturation process of the autophagosome and endosome (Fig. 5*F*).

Discussion

This study elucidated that the NACHT domain of NLRs physically interacts with the ECD of Beclin1 and inhibits induction of the autophagic process. It was shown that Bcl-2 interacts with the Beclin1 BD (24), whereas UVRAG targets the Beclin1 CCD (7). CCD and ECD of Beclin1 are required for its interaction with PI3KC3 and a heterodimer of VPS34/VPS15 (7). However, molecular mechanisms underlying the complex formation of these Beclin1-interacting molecules and their cooperation or competition for the induction of autophagy are largely unknown. Results from our immunoprecipitation assay and gel-filtration analysis indicated that NLRP4 is a component of the 500–700-kDa cytoplasmic complex that contains Beclin1 (Fig. 1*C*, 1*F*). Previous studies and our present data showed that, under physiological conditions, the majority of cellular Beclin1 (52 kDa) complexes with VPS34 (100 kDa) and VPS15 (150 kDa) and that Beclin1 migrate into fractions spanning a relatively broad range of sizes

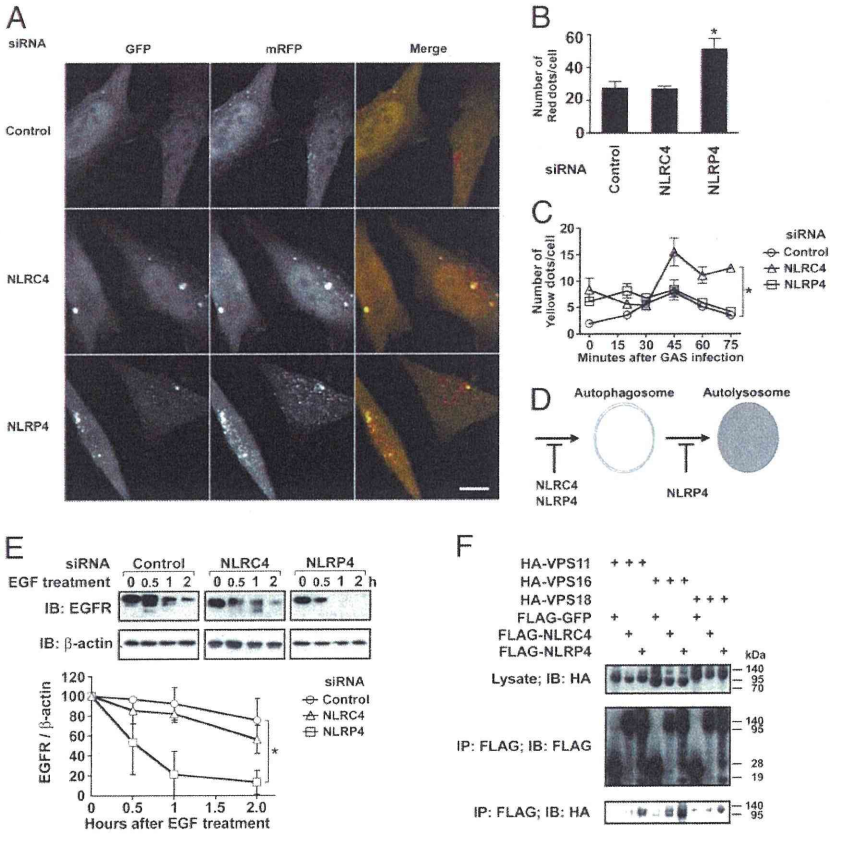

FIGURE 5. NLRP4 controls the maturation of autophagosome and endosome through the association with class C VPS. *A–C*, HeLa cells stably expressing mRFP-GFP-LC3 were transfected with control dsRNA or pooled dsRNAs targeting NLRC4 or NLRP4. *A* and *B*, Forty-eight hours following transfection, the cells were fixed and then analyzed under a confocal microscope. *A*, Representative photomicrographs are shown; scale bar, 20 μm. *B*, The number of red fluorescent dots (>1 μm) in individual cells was counted (n = 10). The graph shows the mean ± SD. *C*, Forty-eight hours after transfection, the cells were infected with GAS at an MOI of 50 for the indicated times, fixed, and analyzed under a confocal microscope. The number of yellow fluorescent dots (>1 μm) in individual cells was counted (n = 10). The graph shows the mean ± SD. *D*, A schematic diagram of target step(s) by NLRC4 or NLRP4 in the course of autophagic flux. *E*, HeLa cells were transfected with control dsRNA or pooled dsRNAs targeting NLRC4 or NLRP4. Forty-eight hours posttransfection, the cells were treated with EGF (200 ng/ml) for the indicated times. The levels of EGFR degradation were examined by immunoblotting analysis. Representative results of at least three independent experiments are shown. The graph shows the mean ± SD. *F*, HEK293 cells were transfected with the indicated plasmids. Forty-eight hours after transfection, the cells were subjected to immunoprecipitation and immunoblotting analyses. Representative results of at least three independent experiments are shown. *$p < 0.05$.

(400–700 kDa). Thus, it was suggested that the Beclin1–PI3KC3 complex (~300 kDa) further interacts with other molecules of different sizes. A recent study revealed that the Atg14L–Beclin1–PI3KC3 complex is required for autophagosome formation, whereas the UVRAG–Beclin1–PI3KC3 complex is crucial for maturation of the autophagosome and endosome. Further interaction of Rubicon with the UVRAG–Beclin1–PI3KC3 complex inhibited the maturation process for the autophagosome and endosome (8). Accordingly, the dynamics of Atg14L, which localizes to the endoplasmic reticulum, isolation membrane, and autophagosome, are different from those of UVRAG and Rubicon, which are present in the endosome and lysosome. Therefore, it was suggested that various types of the Beclin1-containing complex are organized in response to the cellular environment, resulting in the control of autophagic flux, whereas interaction with Rubicon inhibits autophagic flux. Although the present study revealed that NLRP4 is one component of the Beclin1 complex, further studies are required to elucidate which factors control the formation of the NLRP4–Beclin1 complex to negatively regulate autophagy during invasive bacterial infection.

Previous studies characterized the nature of GAS-containing autophagosome-like vacuoles (GcAVs). GcAVs are large (>10 μm) relative to physiological autophagosomes (0.5–1.0 μm) (4). Although GcAVs were shown to be $LC3^+$ and are generated in an Atg5-dependent manner, a recent study suggested that Rab7 recruitment to GcAVs, but not physiological autophagosomes, plays an important role in the formation of GcAVs that is required for elimination of invasive GAS bacteria (25). Because our data showed that the knockdown of NLRP4 increased the number of GcAVs and that NLRP4 interacted with the components of the C-VPS complex linking Rab7 activation, it was strongly suggested that NLRP4 correlates with the activation of Rab7 on GcAVs (Figs. 4*A*, 4*B*, 5*F*).

Several studies investigated the cellular functions of NLRP4, but none of them revealed its biological role associated with bacterial infection (26–28). Another interesting aspect of NLRP4 that we elucidated in this study was the subcellular dynamics of this molecule in response to bacterial infection (i.e., NLRP4 is recruited and accumulated on bacteria-containing phagosomes at an early stage of infection). Previous studies demonstrated that mice deficient for NLRC4 or NLRP3 have defective IL-1β production in response to bacterial components, such as flagellin or LPS. There are no reports showing evidence of the direct interaction between NLRs and bacterial components, although several members of the NLR family were shown to be linked to the bacterial-recognition mechanism (29). Furthermore, it was recently shown that NOD1 and NOD2, the NLR sensors of bacterial peptidoglycan (muramyldipeptide), directly induce autophagy by recruiting Atg16L1 to the phagosomes containing bacteria (30, 31). Accompanying these findings, recent genome-wide association studies revealed that the loss-of-function mutation of the *Atg16l1* gene, as well as the gain-of-function mutation of the *Nod2* gene, are seen at significantly greater rates in patients with Crohn's disease, suggesting that the NLR sensors and autophagy are associated with the pathogenesis of inflammation caused by bacteria (32, 33). The epithelial cell-expressing Atg16L1 T300A mutant, a risk variant of Crohn's disease, undergoes physiological autophagy but is defective for the autophagic process induced by bacterial infection. This would indicate that Atg16L mediates a specific signaling pathway linking bacterial recognition and the initiation of autophagy (34). In fact, a previous study revealed that Atg16L1-deficient murine cells are more susceptible to secreting IL-1β in response to inflammatory stimuli, such as LPS or dextran sulfate sodium (35). Because Atg16L was shown to be an essential factor in the regulation of autophagy downstream of Beclin1-mediated signaling, it was suggested that Atg16L–NOD2 interaction is a crossroad between macroautophagy and inflammasome activation. Because our research also clarified the novel molecular interaction between NLRP4 and Beclin1, we are investigating, in on-going studies, upstream signaling events regulating the association between inflammasome and autophagy.

With regard to autophagy-inducing pathways specific to bacterial infection, it was shown that signaling mediated by TLRs can lead to autophagosome formation (36, 37). Immunity-related p47 guanosine triphosphatase M, a cytoplasmic molecule crucial in the recognition and elimination of invasive pathogens, also mediates the induction of autophagy following *Mycobacterium tuberculosis* infection (38, 39). Several studies have begun to elucidate the mechanisms underlying the pathway linking the sensory machinery of pathogens and the initiation of autophagy. Further genetic studies would determine how NLRP4, directly or indirectly, contributes to the autophagic bactericidal process during invasive bacterial infections and whether NLRP4 regulates inflammasome activation upon invasive bacterial infection with or without other NLR members.

Acknowledgments

We thank Drs. E. Hanski (The Hebrew University-Hadassah Medical School) and H. Miyoshi (RIKEN BioResource Center, Tsukuba, Japan) for providing experimental materials and suggestions and N. Araya for technical assistance.

Disclosures

The authors have no financial conflicts of interest.

References

1. Kuma, A., M. Hatano, M. Matsui, A. Yamamoto, H. Nakaya, T. Yoshimori, Y. Ohsumi, T. Tokuhisa, and N. Mizushima. 2004. The role of autophagy during the early neonatal starvation period. *Nature* 432: 1032–1036.
2. Komatsu, M., S. Waguri, T. Ueno, J. Iwata, S. Murata, I. Tanida, J. Ezaki, N. Mizushima, Y. Ohsumi, Y. Uchiyama, et al. 2005. Impairment of starvation-induced and constitutive autophagy in Atg7-deficient mice. *J. Cell Biol.* 169: 425–434.
3. Nishida, Y., S. Arakawa, K. Fujitani, H. Yamaguchi, T. Mizuta, T. Kanaseki, M. Komatsu, K. Otsu, Y. Tsujimoto, and S. Shimizu. 2009. Discovery of Atg5/Atg7-independent alternative macroautophagy. *Nature* 461: 654–658.
4. Nakagawa, I., A. Amano, N. Mizushima, A. Yamamoto, H. Yamaguchi, T. Kamimoto, A. Nara, J. Funao, M. Nakata, K. Tsuda, et al. 2004. Autophagy defends cells against invading group A *Streptococcus*. *Science* 306: 1037–1040.
5. Birmingham, C. L., V. Canadien, E. Gouin, E. B. Troy, T. Yoshimori, P. Cossart, D. E. Higgins, and J. H. Brumell. 2007. *Listeria monocytogenes* evades killing by autophagy during colonization of host cells. *Autophagy* 3: 442–451.
6. Yoshimori, T., and T. Noda. 2008. Toward unraveling membrane biogenesis in mammalian autophagy. *Curr. Opin. Cell Biol.* 20: 401–407.
7. Liang, C., P. Feng, B. Ku, I. Dotan, D. Canaani, B. H. Oh, and J. U. Jung. 2006. Autophagic and tumour suppressor activity of a novel Beclin1-binding protein UVRAG. *Nat. Cell Biol.* 8: 688–699.
8. Matsunaga, K., T. Saitoh, K. Tabata, H. Omori, T. Satoh, N. Kurotori, I. Maejima, K. Shirahama-Noda, T. Ichimura, T. Isobe, et al. 2009. Two Beclin 1-binding proteins, Atg14L and Rubicon, reciprocally regulate autophagy at different stages. *Nat. Cell Biol.* 11: 385–396.
9. Zhong, Y., Q. J. Wang, X. Li, Y. Yan, J. M. Backer, B. T. Chait, N. Heintz, and Z. Yue. 2009. Distinct regulation of autophagic activity by Atg14L and Rubicon associated with Beclin 1-phosphatidylinositol-3-kinase complex. *Nat. Cell Biol.* 11: 468–476.
10. Liang, C., J. S. Lee, K. S. Inn, M. U. Gack, Q. Li, E. A. Roberts, I. Vergne, V. Deretic, P. Feng, C. Akazawa, and J. U. Jung. 2008. Beclin1-binding UVRAG targets the class C Vps complex to coordinate autophagosome maturation and endocytic trafficking. *Nat. Cell Biol.* 10: 776–787.
11. Wilmanski, J. M., T. Petnicki-Ocwieja, and K. S. Kobayashi. 2008. NLR proteins: integral members of innate immunity and mediators of inflammatory diseases. *J. Leukoc. Biol.* 83: 13–30.
12. Suzuki, T., L. Franchi, C. Toma, H. Ashida, M. Ogawa, Y. Yoshikawa, H. Mimuro, N. Inohara, C. Sasakawa, and G. Nuñez. 2007. Differential regulation of caspase-1 activation, pyroptosis, and autophagy via Ipaf and ASC in *Shigella*-infected macrophages. *PLoS Pathog.* 3: e111.
13. Kobiyama, K., F. Takeshita, N. Jounai, A. Sakaue-Sawano, A. Miyawaki, K. J. Ishii, T. Kawai, S. Sasaki, H. Hirano, N. Ishii, et al. 2010. Extrachromosomal

histone H2B mediates innate antiviral immune responses induced by intracellular double-stranded DNA. *J. Virol.* 84: 822–832.
14. Martinon, F., K. Burns, and J. Tschopp. 2002. The inflammasome: a molecular platform triggering activation of inflammatory caspases and processing of proIL-beta. *Mol. Cell* 10: 417–426.
15. Takeshita, F., K. J. Ishii, K. Kobiyama, Y. Kojima, C. Coban, S. Sasaki, N. Ishii, D. M. Klinman, K. Okuda, S. Akira, and K. Suzuki. 2005. TRAF4 acts as a silencer in TLR-mediated signaling through the association with TRAF6 and TRIF. *Eur. J. Immunol.* 35: 2477–2485.
16. Miyoshi, H., U. Blömer, M. Takahashi, F. H. Gage, and I. M. Verma. 1998. Development of a self-inactivating lentivirus vector. *J. Virol.* 72: 8150–8157.
17. Miyoshi, H., M. Takahashi, F. H. Gage, and I. M. Verma. 1997. Stable and efficient gene transfer into the retina using an HIV-based lentiviral vector. *Proc. Natl. Acad. Sci. USA* 94: 10319–10323.
18. Jounai, N., F. Takeshita, K. Kobiyama, A. Sawano, A. Miyawaki, K. Q. Xin, K. J. Ishii, T. Kawai, S. Akira, K. Suzuki, and K. Okuda. 2007. The Atg5 Atg12 conjugate associates with innate antiviral immune responses. *Proc. Natl. Acad. Sci. USA* 104: 14050–14055.
19. Takeshita, F., K. Suzuki, S. Sasaki, N. Ishii, D. M. Klinman, and K. J. Ishii. 2004. Transcriptional regulation of the human TLR9 gene. *J. Immunol.* 173: 2552–2561.
20. Sakaue-Sawano, A., H. Kurokawa, T. Morimura, A. Hanyu, H. Hama, H. Osawa, S. Kashiwagi, K. Fukami, T. Miyata, H. Miyoshi, et al. 2008. Visualizing spatiotemporal dynamics of multicellular cell-cycle progression. *Cell* 132: 487–498.
21. Geddes, B. J., L. Wang, W. J. Huang, M. Lavellee, G. A. Manji, M. Brown, M. Jurman, J. Cao, J. Morgenstern, S. Merriam, et al. 2001. Human CARD12 is a novel CED4/Apaf-1 family member that induces apoptosis. *Biochem. Biophys. Res. Commun.* 284: 77–82.
22. Komatsu, M., S. Waguri, M. Koike, Y. S. Sou, T. Ueno, T. Hara, N. Mizushima, J. Iwata, J. Ezaki, S. Murata, et al. 2007. Homeostatic levels of p62 control cytoplasmic inclusion body formation in autophagy-deficient mice. *Cell* 131: 1149–1163.
23. Kimura, S., N. Fujita, T. Noda, and T. Yoshimori. 2009. Monitoring autophagy in mammalian cultured cells through the dynamics of LC3. *Methods Enzymol.* 452: 1–12.
24. Pattingre, S., A. Tassa, X. Qu, R. Garuti, X. H. Liang, N. Mizushima, M. Packer, M. D. Schneider, and B. Levine. 2005. Bcl-2 antiapoptotic proteins inhibit Beclin 1-dependent autophagy. *Cell* 122: 927–939.
25. Yamaguchi, H., I. Nakagawa, A. Yamamoto, A. Amano, T. Noda, and T. Yoshimori. 2009. An initial step of GAS-containing autophagosome-like vacuoles formation requires Rab7. *PLoS Pathog.* 5: e1000670.
26. Grenier, J. M., L. Wang, G. A. Manji, W. J. Huang, A. Al-Garawi, R. Kelly, A. Carlson, S. Merriam, J. M. Lora, M. Briskin, et al. 2002. Functional screening of five PYPAF family members identifies PYPAF5 as a novel regulator of NF-kappaB and caspase-1. *FEBS Lett.* 530: 73–78.
27. Fiorentino, L., C. Stehlik, V. Oliveira, M. E. Ariza, A. Godzik, and J. C. Reed. 2002. A novel PAAD-containing protein that modulates NF-kappa B induction by cytokines tumor necrosis factor-alpha and interleukin-1beta. *J. Biol. Chem.* 277: 35333–35340.
28. Zhang, P., M. Dixon, M. Zucchelli, F. Hambiliki, L. Levkov, O. Hovatta, and J. Kere. 2008. Expression analysis of the NLRP gene family suggests a role in human preimplantation development. *PLoS ONE* 3: e2755.
29. Hise, A. G., J. Tomalka, S. Ganesan, K. Patel, B. A. Hall, G. D. Brown, and K. A. Fitzgerald. 2009. An essential role for the NLRP3 inflammasome in host defense against the human fungal pathogen *Candida albicans*. *Cell Host Microbe* 5: 487–497.
30. Travassos, L. H., L. A. Carneiro, M. Ramjeet, S. Hussey, Y. G. Kim, J. G. Magalhaes, L. Yuan, F. Soares, E. Chea, L. Le Bourhis, et al. 2010. Nod1 and Nod2 direct autophagy by recruiting ATG16L1 to the plasma membrane at the site of bacterial entry. *Nat. Immunol.* 11: 55–62.
31. Cooney, R., J. Baker, O. Brain, B. Danis, T. Pichulik, P. Allan, D. J. Ferguson, B. J. Campbell, D. Jewell, and A. Simmons. 2010. NOD2 stimulation induces autophagy in dendritic cells influencing bacterial handling and antigen presentation. *Nat. Med.* 16: 90–97.
32. Abbott, D. W., A. Wilkins, J. M. Asara, and L. C. Cantley. 2004. The Crohn's disease protein, NOD2, requires RIP2 in order to induce ubiquitinylation of a novel site on NEMO. *Curr. Biol.* 14: 2217–2227.
33. Hampe, J., A. Franke, P. Rosenstiel, A. Till, M. Teuber, K. Huse, M. Albrecht, G. Mayr, F. M. De La Vega, J. Briggs, et al. 2007. A genome-wide association scan of nonsynonymous SNPs identifies a susceptibility variant for Crohn disease in ATG16L1. *Nat. Genet.* 39: 207–211.
34. Kuballa, P., A. Huett, J. D. Rioux, M. J. Daly, and R. J. Xavier. 2008. Impaired autophagy of an intracellular pathogen induced by a Crohn's disease associated ATG16L1 variant. *PLoS ONE* 3: e3391.
35. Saitoh, T., N. Fujita, M. H. Jang, S. Uematsu, B. G. Yang, T. Satoh, H. Omori, T. Noda, N. Yamamoto, M. Komatsu, et al. 2008. Loss of the autophagy protein Atg16L1 enhances endotoxin-induced IL-1beta production. *Nature* 456: 264–268.
36. Delgado, M. A., R. A. Elmaoued, A. S. Davis, G. Kyei, and V. Deretic. 2008. Toll-like receptors control autophagy. *EMBO J.* 27: 1110–1121.
37. Xu, Y., C. Jagannath, X. D. Liu, A. Sharafkhaneh, K. E. Kolodziejska, and N. T. Eissa. 2007. Toll-like receptor 4 is a sensor for autophagy associated with innate immunity. *Immunity* 27: 135–144.
38. MacMicking, J. D., G. A. Taylor, and J. D. McKinney. 2003. Immune control of tuberculosis by IFN-gamma-inducible LRG-47. *Science* 302: 654–659.
39. Singh, S. B., A. S. Davis, G. A. Taylor, and V. Deretic. 2006. Human IRGM induces autophagy to eliminate intracellular mycobacteria. *Science* 313: 1438–1441.

Supplemental Data

Supplemental Table I. Sequences of dsRNA for knockdown of *NLRC4* or *NLRP4*.

Name	RNA sequence
NLRC4-1	Sense 5'-AAAUGGAUGCCACACUCUACAAAGG-3' Antisense 5'-CCUUUGUAGAGUGUGGCAUCCAUUU-3'
NLRC4-2	Sense 5'-UAUACUUUGGCUUGAACCUUUGAGC-3' Antisense 5'-GCUCAAAGGUUCAAGCCAAAGUAUA-3'
NLRC4-3	Sense 5'-CAAAGAAGUCAAAUAAGUAAUCGGG-3' Antisense 5'-CCCGAUUACUUAUUUGACUUCUUUG-3'
NLRP4-1	Sense 5'-UUCAAGGCAUCACAGAGGGACCUGA-3' Antisense 5'-UCAGGUCCCUCUGUGAUGCCUUGAA-3'
NLRP4-2	Sense 5'-UCUUACUGCAGGUGAGAACAGACGC-3' Antisense 5'-GCGUCUGUUCUCACCUGCAGUAAGA-3'
NLRP4-3	Sense 5'-UUCAAGGUCAGGUUGAGCUGCUGCA-3' Antisense 5'-UGCAGCAGCUCAACCUGACCUUGAA-3'

Supplemental Table II. Sequences of DNA primers to investigate the knockdown efficiency of NLRC4 or NLRP4 siRNA.

Name	DNA sequence
NLRC4 (300-760 bp)	Sense 5'-TTGGCTCAGGATTTAAAGGAC-3' Antisense 5'-TGAATTCATTGTAGCCATCAAG-3'
NLRP4 (957 -1557 bp)	Sense 5'- AAGAGCCATGGAAGCCTTCAATC -3' Antisense 5'-AAAAAACGCATCCAGTTTTTCTTG-3'

Supplemental Table III. Sequences of DNA primers to investigate the RNA levels encoding *NLRC4* or *NLRP4*.

Name	DNA sequence
gapdh	Sense 5'- GCCTTCCGTGTCCCCACTGC -3' Antisense 5'- CAATGCCAGCCCCAGCGTCA -3'
NLRC4#1	Sense 5'- GCGTGGAGCAGCTGACCCTG -3' Antisense 5'- GGCCCTGCTGAGACGGAGGA -3'
NLRC4#2	Sense 5'- ATGCTGCTGAAGCTGCGGCA -3' Antisense 5'- TGAGAGCCTGGGCGCTGTCT -3'
NLRP4#1	Sense 5'- CCAGCACCAGCTGAAGGCCC -3' Antisense 5'- AGGAGCTCTCACGCTCCCCG -3'
NLRP4#2	Sense 5'- GGCGGCTTGAACGAACCCGA -3' Antisense 5'- GAGCTCCTTCGGGCACACGG -3'

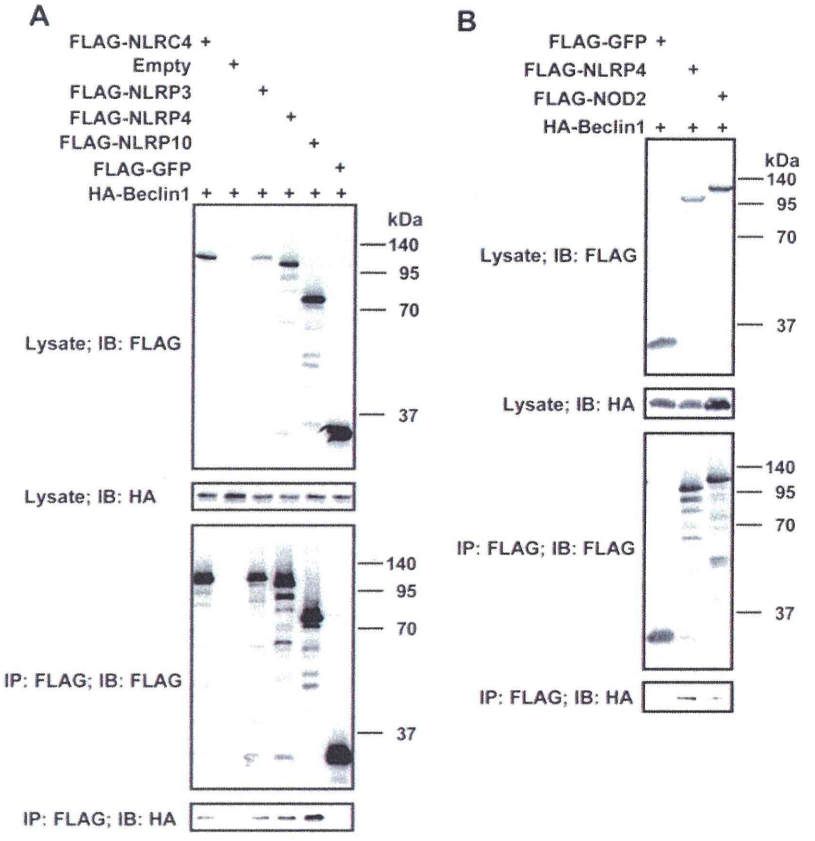

Supplemental Figure 1. NLRC4, NLRP3, 4, 10 and NOD2 interact with Beclin1 in HeLa cells.

A and *B*, HeLa cells were transfected with the indicated plasmids. Forty-eight hours post-transfection, cells were subjected to immunoprecipitation and immunoblotting analyses.

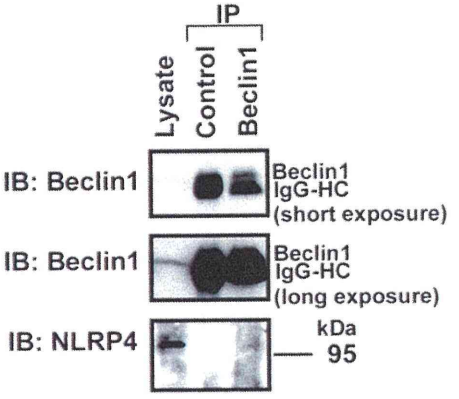

Supplemental Figure 2. NLRP4 associates with Beclin1 in HuVECs under physiological condition.

The two millions of HuVECs were lysed, and endogenous Beclin1 was immunoprecipitated, and then the associated levels of NLRP4 were evaluated by immunoblotting.